EFFECT OF IONIC STRENGTH AND SALT TYPE ON HUMIC ACID FOULING OF FORWARD OSMOSIS MEMBRANES

A Senior Honors Thesis

Presented in Partial Fulfillment of the Requirements for Graduation with Distinction in the Department of Mechanical Engineering in the Undergraduate Colleges at

The Ohio State University

By

Adam Millat

The Ohio State University

25 October 2011

Examination Committee: Approval:

Dr. Shaurya Prakash, Advisor _____

Dr. A. Terrence Conlisk Jr. _____

Abstract

The effect of ionic strength and salt type on humic acid (HA) fouling of forward osmosis membranes was systematically investigated. A permeation cell was used to produce an osmotic flow of working solution from the dilute HA feed solution to the concentrated draw solution. Two forward osmosis membranes were tested to determine the dependence of fouling on membrane type. A nanocapillary array membrane with nominal pore size of 10 nm was also used but did not produce an osmotic flow due to the diffusion of salts through the larger membrane pores. 0.5 mM and 5.0 mM KCl and $CaCl_2$ feed solutions were used to determine the effect of ionic strength and salt type on humic acid fouling. Average flux data from baseline experiments with zero HA was compared to average flux data from experiments containing 10 mg/L of HA, with no measurable effect observed. Ionic strength of the feed solution was shown to affect the average trans-membrane water flux with higher average fluxes found for the 0.5 mM feed solution compared to the 5.0 mM feed solution. Salt type was shown to affect the average trans-membrane water flux and was found to be dependent on the membrane type. Internal concentration polarization was determined to be the primary cause for decreased average fluxes at high ionic strengths, while HA fouling was determined to depend on the composition of the working solution. Despite not always having higher initial average fluxes, $CaCl_2$ working solutions always resulted in larger percent reductions of average flux which could be evidence of increased HA fouling in the presence of Ca^{2+} ions. This result agrees with previous findings of HA fouling in membrane processes.

Dedication

This work is dedicated to my parents, for all their support in getting me to where I'm at today.

Acknowledgements

I would like to acknowledge and thank my research advisor Dr. Shaurya Prakash for his patience, guidance, and wisdom throughout the course of this project. I would also like to extend a thank you to Ms. Karen Bellman and the rest of the researchers at the Microsystems and Nanosystems (MSNS) Lab for their help in training me. Financial support or in-kind services were provided by the following institutions and companies: the Engineering Experiment Station at the Ohio State University, the Ohio State University College of Engineering, the MSNS Lab, and Hydration Technology Innovations.

Table of Contents

List of Figures

List of Tables

List of Equations

1. INTRODUCTION

1.1 PURPOSE

Membrane fouling is the build-up and adsorption of particles on the membrane surface and in the membrane pores. Membrane fouling results in significantly increased operational costs, decreased trans-membrane flux, and decreased permeate consistency. The purpose of this project is to characterize the effect of solution composition on humic acid (HA) fouling of forward osmosis membranes. Specifically, this project seeks to answer two questions:

i. How does salt type and ionic strength affect water flux through forward osmosis membranes in the presence of HA?
ii. How do results in a dead-end flow setup compare with previous studies in cross-flow setups?

1.2 WATER AND THE WORLD – TODAY

The scarcity of freshwater supplies has become one of the world's most pressing problems, and society's ability to efficiently purify and distribute water will be a large predictor of the world's ability to thrive. Although about 70% of planet Earth is covered in water only 2.5% of the planet's water supply is freshwater; see Figure 1.1. Moreover, of all the world's freshwater, nearly 70% is locked up in ice and snow in mountainous regions and is thus practically unusable; see Figure 1.2. Total U.S withdrawals of water are estimated at 124T gallons/year, which is roughly equivalent to the 130T gallon yearly outflow of the Mississippi basin [1].

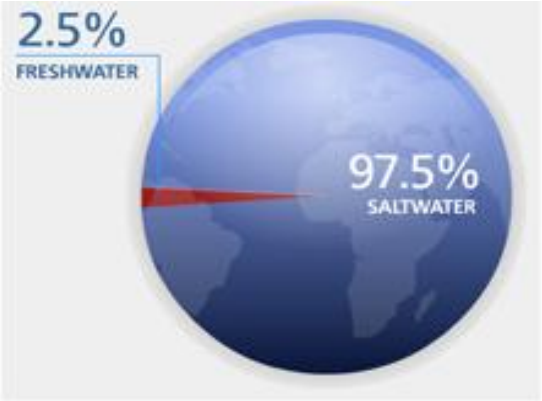

Figure 1.1: Total world water [2].

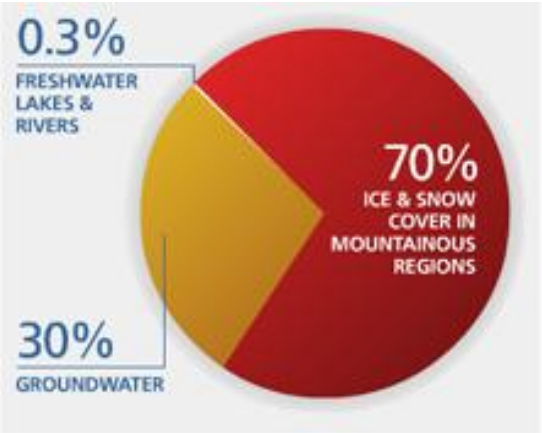

Figure 1.2: Breakdown of freshwater resources [2].

For one out of every six people in the world—about 1.1B people—these statistics materialize into a lack of access to safe water. Combined with the lack of basic sanitation that is experienced by 2.6B people worldwide, the current water situation leads to the death of 1.6M children a year due to diarrhoeal diseases alone, which could be largely prevented by simply washing hands with soap and water [3].

Additionally, the world relies on clean water for much more than just drinking. In fact, only 8% of the freshwater that the world uses is for domestic uses; see Figure 1.3. Water is used heavily in industrial processes and irrigation where it often becomes contaminated with industrial waste, pharmaceuticals, and pesticides which further complicate the purification process needed to properly dispose of the waste and recycle the water. As many of these industrial processes

include the production of energy, it becomes clear that issues of water and energy are intrinsically linked. This is evident in that it takes 4 – 6 gallons of water to refine just one gallon of ethanol and it takes about 1000 times more to irrigate the land for the corn used to produce that gallon [1].

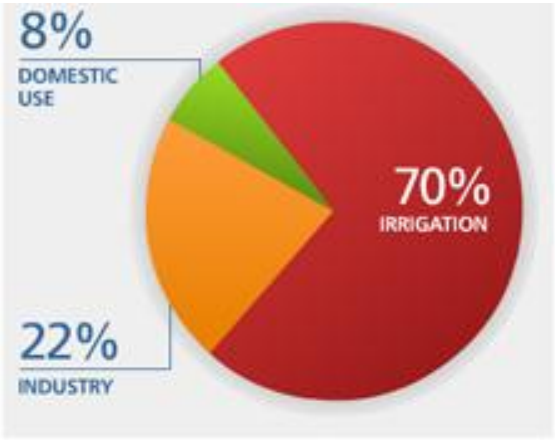

Figure 1.3: Breakdown of freshwater use [2].

1.3 Water and the World – Tomorrow

With billions of people living in water-stressed areas today the outlook for the world's water situation does not look great. In fact, water use has increased at greater than twice the rate of population increase in the last century [2]. Moreover, developing countries are at a greater risk as water withdrawals in developing countries are predicted to increase by 50% in 2025, compared to a still sizeable 18% in developed countries [2]. This is further complicated by the over 145 countries that have territory within a transboundary basin, setting water up to be a highly contested resource and a possible source of conflict [2]. Fortunately, large amounts of capital—both human and physical—are devoted to solving this problem.

1.4 Types of Water

Water can be classified according to its salinity into three general groups. Potable water contains 0.020 mg/L of total dissolved solids (TDS), whereas seawater contains 35000 mg/L

TDS [4]. Brackish water is often found in underground aquifers or where freshwater and seawater meet and thus contains an intermediate amount of TDS; see Table 1.1.

Table 1.1: Salinity and pH of water types.

	Potable water [4]:	Brackish water:	Seawater:
Salinity (mg/L)	0.020	Largely source dependent	35000
pH	6.5-8.5	Largely source dependent	7.5-8.4

1.5 Current Purification Methods

Current water purification methods may be classified as temperature-driven distillation processes and membrane-based processes.

1.5.1 Distillation Processes

Distillation processes operate by using a heat source to evaporate the source water which gravimetrically leaves dissolved salts behind. The water vapor is then condensed separately from the salts resulting in freshwater. The distillation process is seen as energy intensive, often requiring up to 25 kWh of energy to produce 1 m^3 of water, however this number has continued to fall due to improvement in plant design including brine recycling. Distillation plants are still widely used today, particularly in the Middle East because they adequately remove the high concentrations of salts found in the Persian Gulf [5]. Moreover, distillation processes are naturally equipped to take advantage of waste heat sources from energy generation through a process called cogeneration. Cogeneration optimizes the energy generation and fresh water production processes by using the low-grade waste heat from power plants to power the water distillation plant. Cogeneration plants have become popular due to the world's increasing demand for energy generation and fresh water production.

Fouling in distillation processes includes both macro- and micro-fouling. Macro-fouling is the build-up of algae and mussels in the reject section where seawater flows. Micro-fouling and corrosion occur in the brine heater often in the form of scaling by calcium- and magnesium-based compounds. Filtering, chlorination, and on-load ball cleaning have proven to be successful countermeasures [14].

A common distillation plant used today is the multiple stage flash distillation plant which operates by condensing water vapor in a series of flash chambers that decrease in temperature and pressure; see Figure 1.4. Incoming seawater is preheated by condensing distillate water vapor which is collected as the final distillate. The preheated seawater is then heated through an evaporator and pumped through the flash chambers where it will evaporate and condense. The brine is extracted from the final flash chamber as waste.

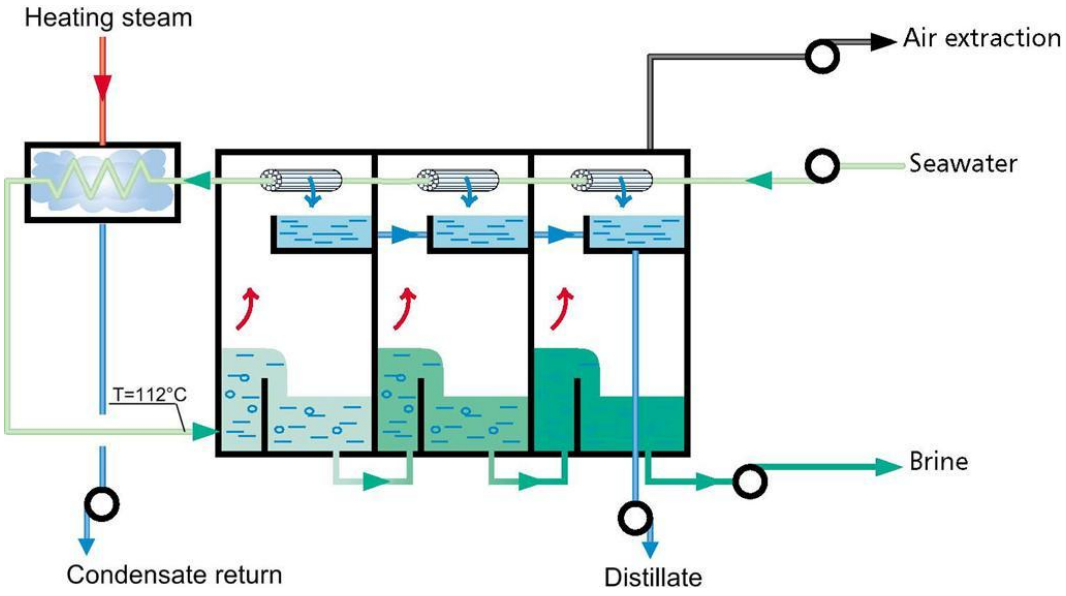

Figure 1.4: Multiple stage flash distillation plant [6].

1.5.2 Membrane-Based Processes

Membrane-based water purification processes use a membrane to separate water from colloids, organic molecules, viruses, and dissolved ions. Membrane-based processes can be

classified into pressure-driven processes (e.g. reverse osmosis), electrically-driven processes (e.g. electrodialysis), or chemical potential-driven processes (e.g. forward osmosis).

Pressure-driven processes include microfiltration, ultrafiltration, nanofiltration, and reverse osmosis (RO), with RO being the only process capable of removing dissolved sodium and chloride ions. These four processes differ solely in the particle size that they allow to translocate across the membrane; see Figure 1.5. RO uses a membrane that excludes nearly all solutes but passes water thus reversing the natural or forward osmosis (FO) process. RO is able to produce potable water of similar quality to that of distillation processes at about a tenth of the energetic cost. RO requires 1.5 to 2.5 kWh of energy to produce 1 m^3 of water, compared to 25 kWh required by most distillation processes for the same volume of water [5]. Typical RO processes require pressure differences of 3 – 6 MPa (approximately 30 – 60 atm) with typical fluxes around 30 L/m^2hr.

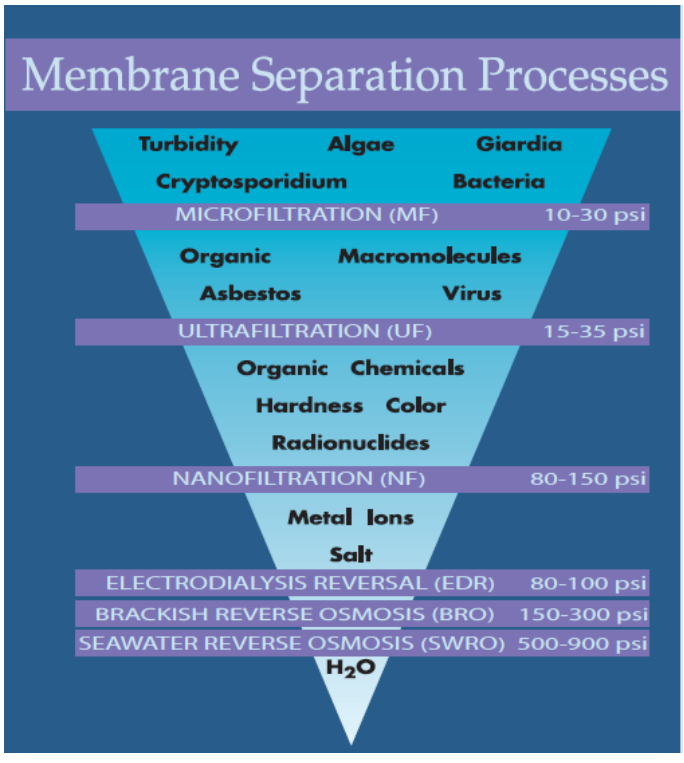

Figure 1.5: Membrane separation processes [7].

Forward osmosis (FO) is a natural process that occurs when there exists a chemical potential gradient across a semi-permeable membrane. Practically, the chemical potential gradient is created by a heavily concentrated draw solution (DS) and less concentrated feed solution (FS) which causes water to flow from the FS to the DS. The osmotic pressure of a solution is a colligative property and refers to the pressure that when applied to a concentrated solution stops the flow of pure water through a semipermeable membrane into the DS. Typical fluxes of pure water into a 45% glucose solution of 10-14 L/m^2hr can be achieved [16]. The flow potential can be quantified by determining the osmotic pressure difference across the membrane according to the van 't Hoff Equation; see Equation 1-1. The van't Hoff factor measures the effect of solute dissociation on colligative properties. For ideal electrolyte solutions, it is equal to the number of discrete ions in a formula unit; however ion pairing often leads to a smaller van't Hoff factor especially for multivalent ions and high concentrations. The direction of solvent flow for RO and FO is opposite; see Figure 1.6.

$$\mathbf{\Delta\Pi = iRT[M_{DS} - M_{FS}]} \qquad 1\text{-}1$$

$\Delta\Pi$ = osmotic pressure difference across membrane

i = van't Hoff factor

R = universal gas constant

T = absolute temperature

M = molarity of solution

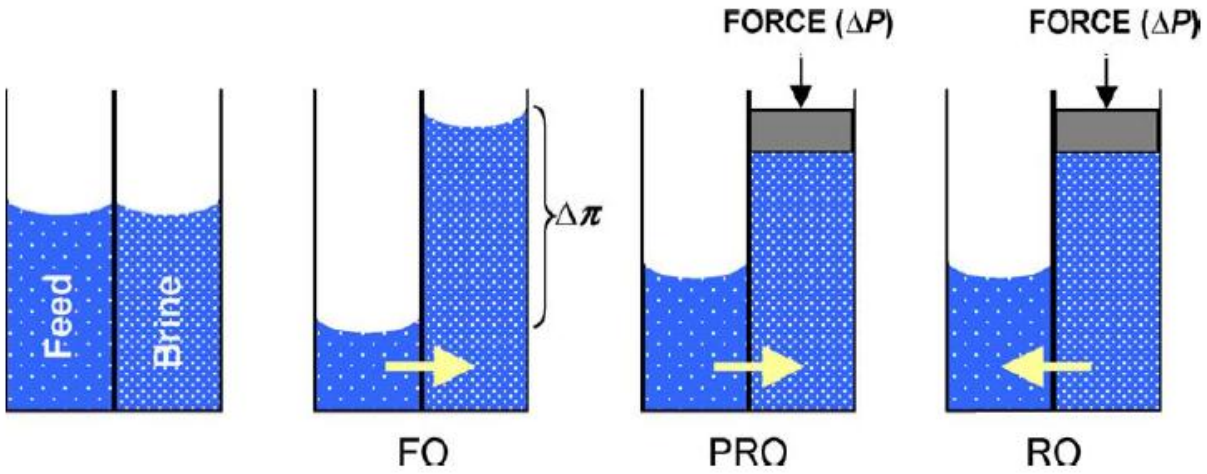

Figure 1.6: Direction of solvent flow in RO, PRO, and FO processes. In PRO, $\Delta\pi > \Delta P$, in RO, $\Delta P > \Delta\pi$ [8].

Although FO cannot produce potable water without the use of secondary processes, there exists a myriad of applications of FO including waste-water concentration, desalination, emergency situations, and energy generation. FO is used to concentrate industrial waste-water and landfill leachate by drawing the water out of these solutions with a heavily concentrated sodium chloride solution. Water recoveries of greater than 90% have been reported [8].

FO desalination applications are primarily focused on the use of draw solutions containing highly soluble ammonia and carbon dioxide gases. These draw solutions pull water from a FS containing either seawater or brackish water. After moderate heating near 60°C the DS breaks down to ammonia and carbon dioxide which can then be readily removed by a distillation process [8].

Hydration bags are used in emergency and military situations to brew a glucose-based sports drink. The bag itself is a FO membrane that uses a glucose DS to pull water from the environment (e.g. ocean, river, puddle) into the bag. Fluxes high enough to produce a 0.35L (12 oz) beverage in 3 hours can be achieved [8].

Although not used to purify water, another application of FO membranes worthy of mention is pressure-retarded osmosis (PRO). PRO uses FO to pressurize the DS, a portion of which pressure is then used to generate power from a turbine; see Figure 1.7. PRO's desirable traits include it is a large renewable resource, has minimal environmental impact, and a high power density. Potential global power production from PRO has been estimated around 2000 TWh per annum [8].

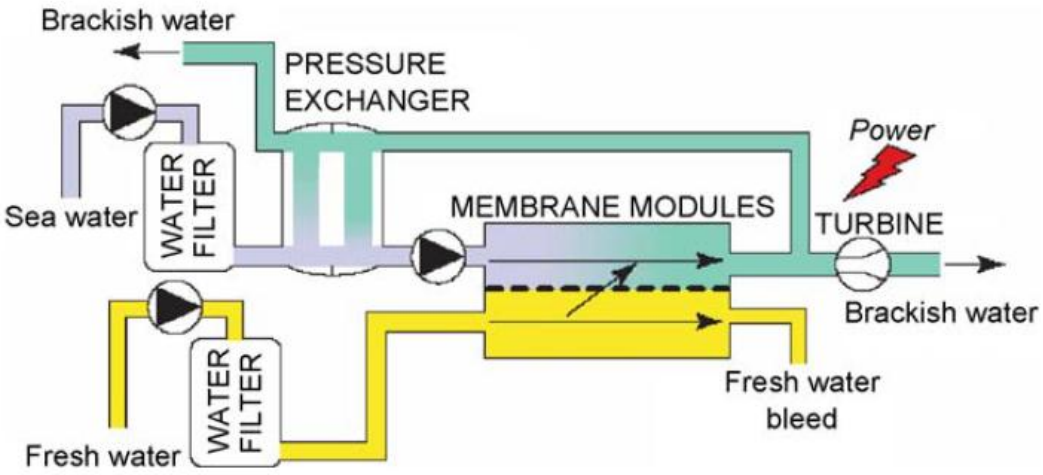

Figure 1.7: PRO power plant process layout [8].

1.6 Fouling in Membrane-Based Processes

Membrane fouling is generally classified into three types based on foulant composition: organic fouling is caused by the build-up of natural organic matter (NOM), bio-fouling refers to the fouling of a membrane by microbial growth, and scaling is the build-up of a cake-like layer often composed of salts or colloids. Organic fouling is more likely to occur at initial membrane stages where the molecules first interact with the membrane surface. Scaling usually occurs in the final membrane stages where the concentration of inorganic salts exceeds the solubility limit due to concentration polarization, causing the salts to precipitate and adsorb on the membrane surface [12]. The term fouling usually refers specifically to organic fouling or bio-fouling but may also include scaling.

A common organic fouling agent found in a wide variety of source waters is humic acid. Humic acid (HA) is a naturally occurring recalcitrant natural organic matter (NOM) with physical properties that vary greatly depending on the source. Essentially decayed plant matter, HA is found in natural waters and wastewater effluents alike. HA has a molecular weight that typically spans hundreds of thousands of Daltons depending on its source [9]. HA fouling has been extensively studied in ultrafiltration, nanofiltration, RO, and FO membranes [9 – 11]. Tang *et al*. systematically studied the effects of solution composition and hydrodynamic conditions on the fouling of RO and nanofiltration membranes by humic acid [9]. Their results overwhelmingly demonstrate the influence of the electrostatic force between the membrane and the HA molecules on membrane fouling, and that the electrostatic force is largely controlled by manipulation of solution composition. They found that severe flux reduction occurred at high initial flux, low pH, and high calcium concentration, while humic acid concentration, ionic strength, and cross-flow velocity only moderately affected flux performance.

pH affects fouling by altering the charge density of HA molecules [9, 12]. At lower pH near the isoelectric point of HA the surface charge density approaches zero; see Figure 1.8. This causes a lower electrostatic repulsion between the HA molecules and the membrane surface, which generally also obtains a negative surface charge in electrolyte solutions. This decreased repulsion results in a greater number of collisions between the HA and the membrane and thus increased fouling; see Figure 1.9.

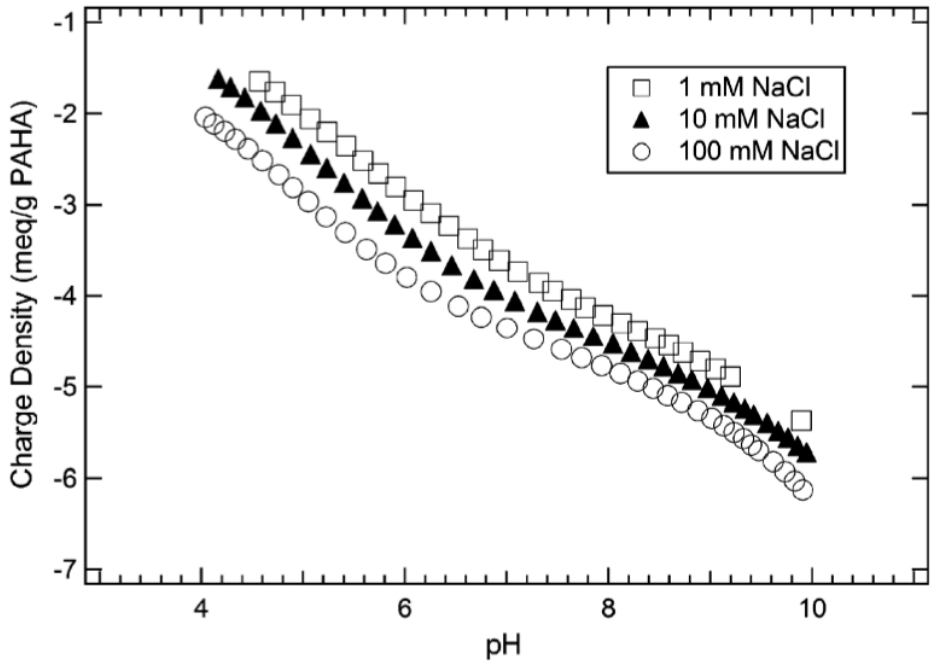

Figure 1.8: HA charge density as a function of solution pH [9]. Note: meq represents 1/1000 of the amount of substance required to combine with 1 mole of hydrogen ions.

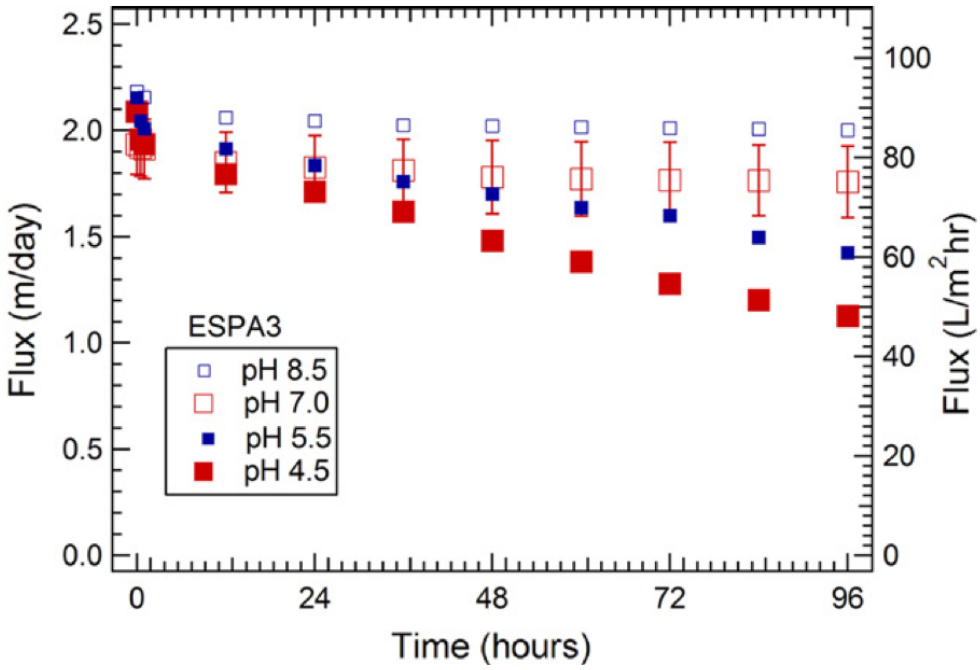

Figure 1.9: Water flux as a function of time and solution pH [9]. Note: units of m/day, from m^3/m^2day.

Similarly, the addition of divalent ions in the source water resulted in higher fouling; see Figure 1.10 [9, 12]. The presence of calcium (Ca^{2+}) in the electrolyte solution reduced the electrostatic repulsion between the HA molecules and the membrane by screening the charge interaction. It was also believed that the calcium ions could physically bridge the HA molecules thus resulting in a higher entropic cost for the HA molecules to enter the membrane.

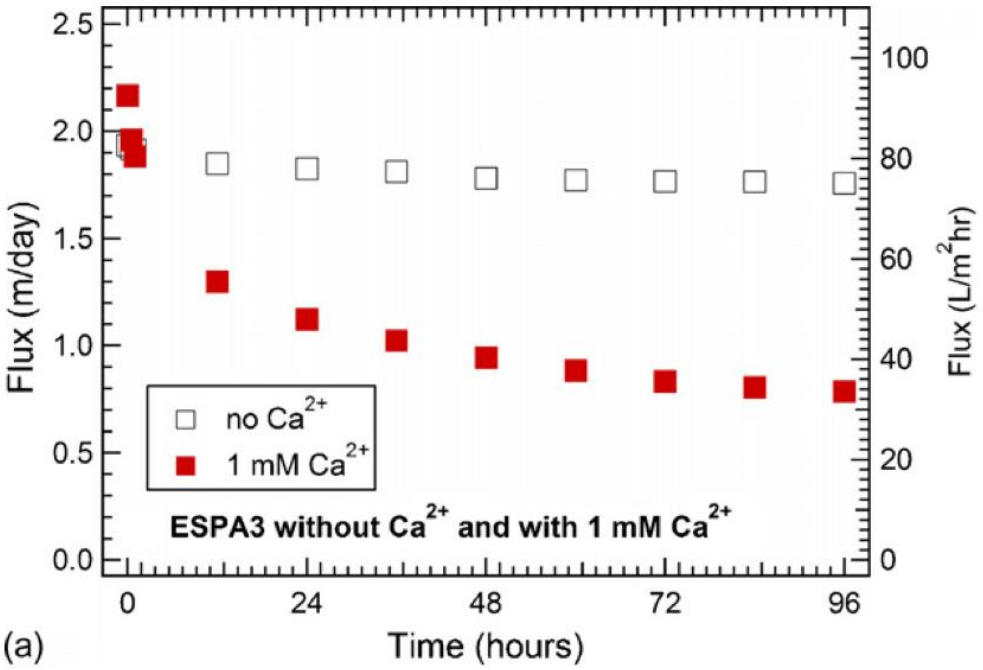

Figure 1.10: Water flux as a function of time and calcium concentration [9].

The primary hydrodynamic condition that promoted membrane fouling was high initial flux [9]. HA foulant layers formed at higher initial flux were considerably denser and thicker. There appeared to be a critical flux below which membrane fouling remained relatively stable as demonstrated by RO membrane ESPA3 which showed flux reductions less than 10% at 689.5 kPa and 1379 kPa but greater than 30% at 2758 kPa.; see Figure 1.11.

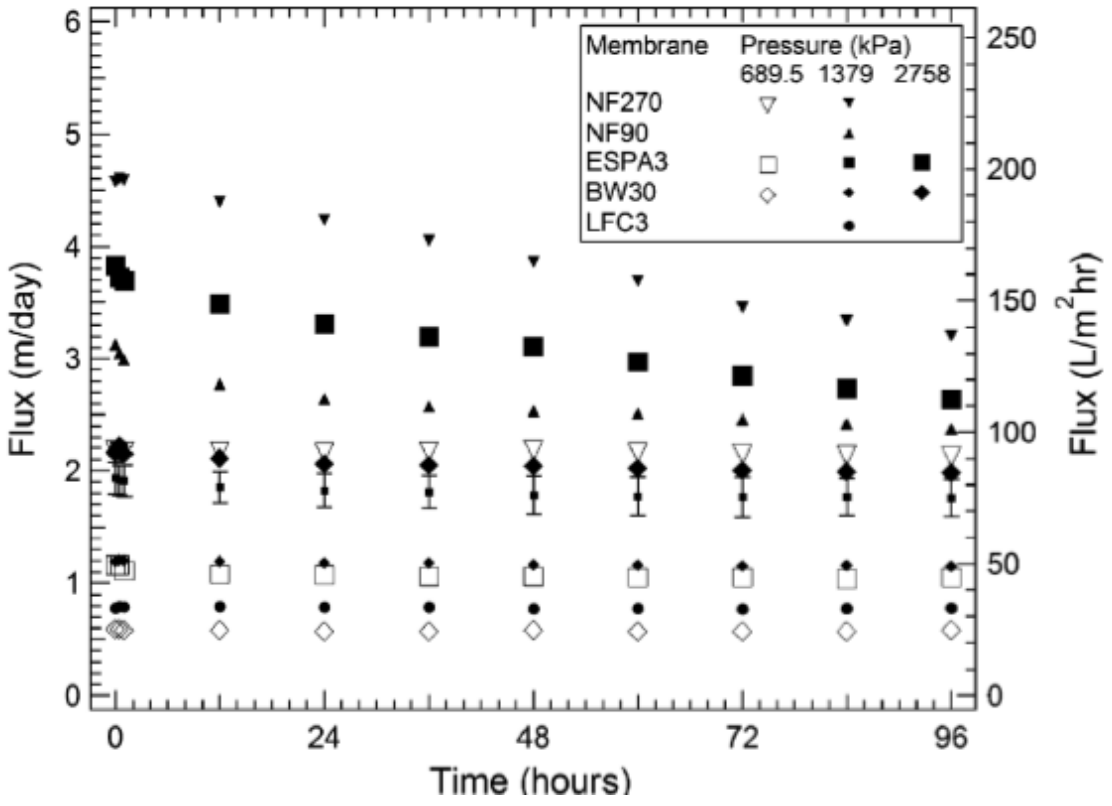

Figure 1.11: Water flux as a function of time for various initial fluxes (pressures) and membranes [9].

1.7 Concentration Polarization in Forward Osmosis

External concentration polarization (ECP) in a pressure-driven membrane process is the build-up of solute particle on either side of the membrane. The build-up causes the localized solute concentration in the immediate region around the membrane to be greater than the bulk concentration and as a result increases the osmotic pressure opposing the pressure-driven flow. Forward osmosis processes are subject to not only external concentration polarization but also internal concentration polarization (ICP) which occurs inside the membrane support layer. Concentrative ICP occurs when the support layer faces the feed solution and is the build-up of solute concentration in the support layer due to FS flow. Dilutive ICP occurs when the support layer faces the draw solution and is the dilution of the draw solution in the membrane support layer due to water flux from the feed solution [8]. Both ECP and ICP rapidly decrease permeate

flux, although ECP can more readily be mitigated by introducing turbulence into the flow adjacent to the membrane surface. A schematic of concentrative and dilutive ICP is shown in Figure 1.12.

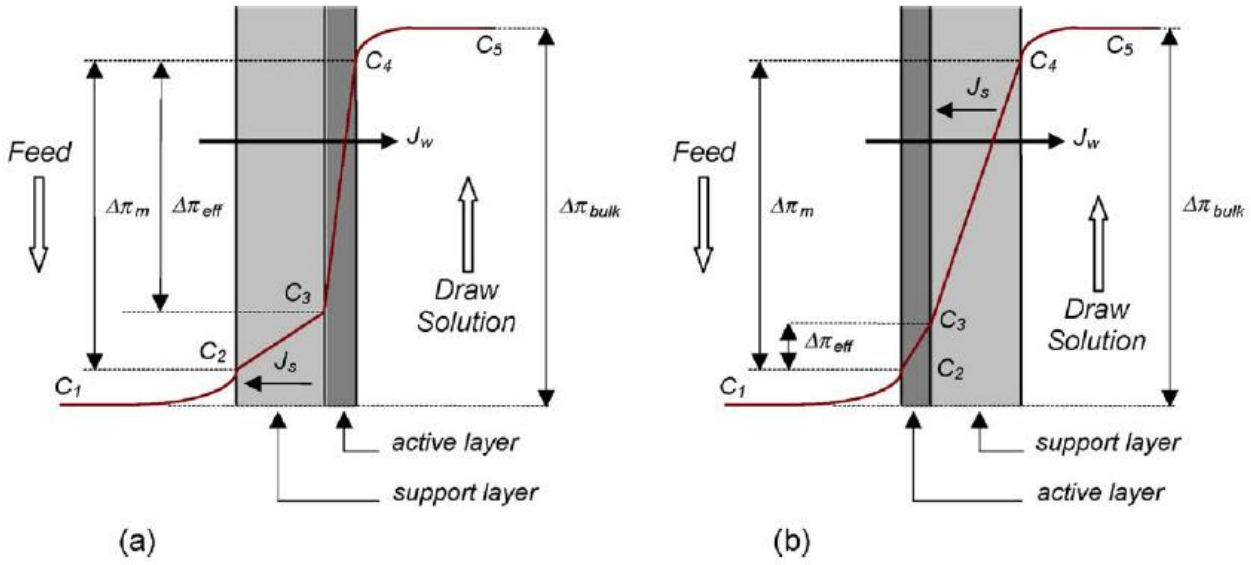

Figure 1.12: Concentrative (a) and dilutive (b) ICP. $\Delta\pi_{bulk}$ is bulk osmotic pressure difference, $\Delta\pi_m$is the membrane osmotic pressure difference (less than $\Delta\pi_{bulk}$ due to ECP), $\Delta\pi_{eff}$ is the effective osmotic pressure difference across the membrane active layer (less than $\Delta\pi_m$due to ICP) [8].

1.8 MULTIVALENT ELECTROLYTE SOLUTIONS

Electrophoresis is the motion of a charged particle relative to the bulk fluid motion [17]. Multivalent electrolyte solutions have been shown to cause a linear decrease in electrophoretic mobility with increasing valence [17]. Although electrophoresis is not the transport mechanism in the experimental system described in this research, this result is worthy of mention because of the possible correlation with the experimental results presented in this research.

2. MATERIALS AND METHODS

All experiments were performed in a dead-end flow permeation cell as shown in Figure 2.1 and the corresponding digital photograph in Figure 2.2. The permeation cell is made of machined acrylic sheets 6.35 mm thick (8560K265, McMaster-Carr) assembled with industrial-strength acrylic glue. Each side of the permeation cell was filled 500 mL of working fluid.

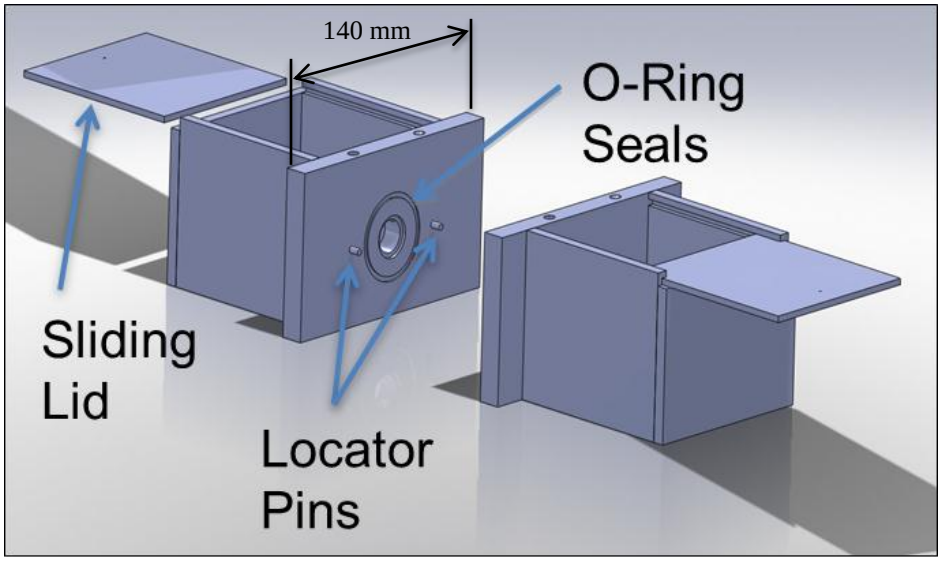

Figure 2.1: Solid model of permeation cell.

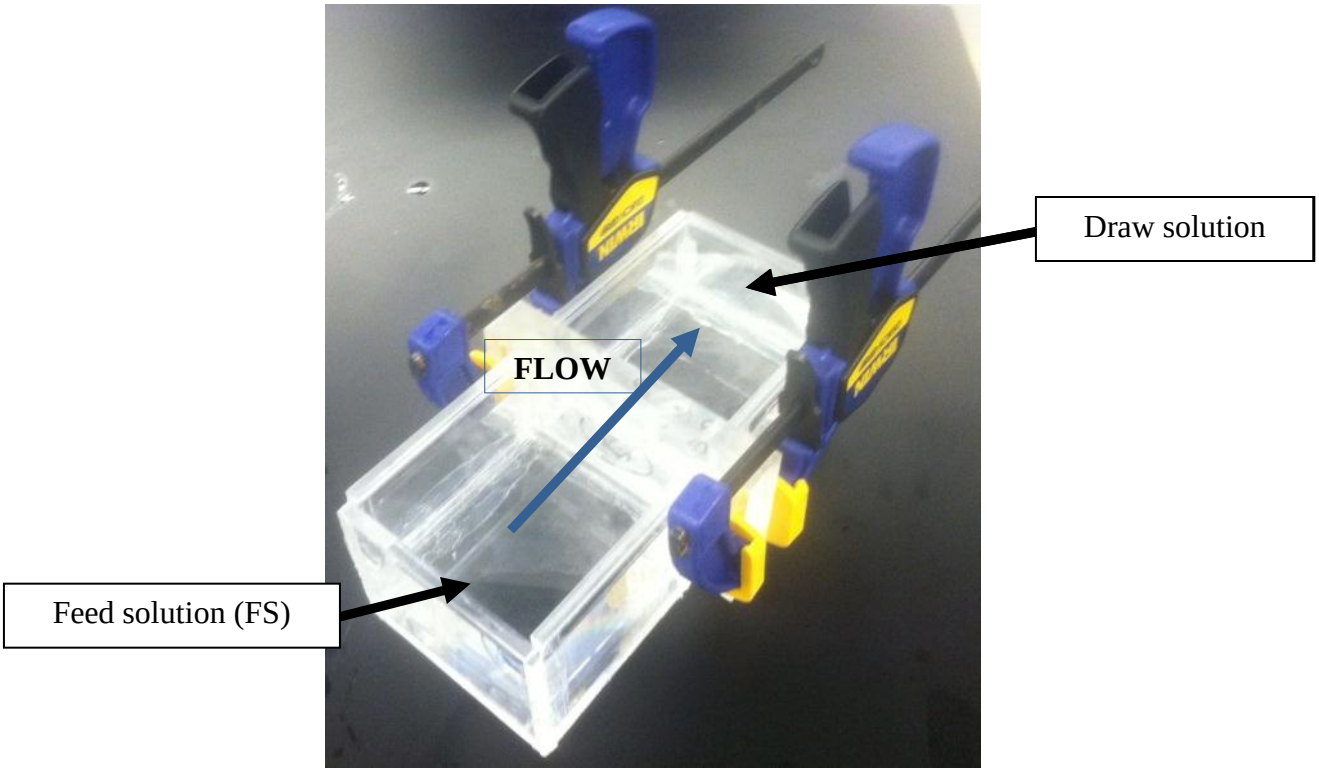

Figure 2.2: Photo of experimental setup.

2.1 Humic Acid Experiments

2.1.1 Experimental Overview

The HA experiments used a heavily concentrated draw solution (DS) to pull water through the membrane from the feed solution (FS). The FS consisted of a weak concentration of the background electrolyte and either 0 mg/L of HA (baseline experiments) or 10 mg/L of HA. The flow of the FS would cause HA-membrane interaction and allow for the characterization of membrane fouling. Conductivity measurements (Accumet AP85 conductivity meter) and water flux measurements (physical height scale) were taken approximately every four hours. To avoid membrane dehydration the FS was always introduced into the device first.

An experimental matrix was designed to characterize HA fouling of the membranes; see Table 2.1. The background electrolyte, FS electrolyte concentration, and membrane were varied to determine the effects of these parameters on HA fouling. All experiments were run for

approximately 24 hours. The nominal osmotic pressure difference across the membrane was held constant for all experiments to 9.780 MPa (~97 atm) regardless of background electrolyte and FS concentration; see Equation 1-1.

Table 2.1: HA experimental matrix.

Index	Salt	FS Conc. (mM)	DS Conc. (M)	Membrane	Duration (hr)	HA Conc. (mg/L)
1	KCl	0.5	2.0000	10 nm NCAM	24	0
2	KCl	5.0	2.0045	10 nm NCAM	24	0
3	KCl	0.5	2.0000	HTI ES-2	24	0
4	KCl	5.0	2.0045	HTI ES-2	24	0
5	KCl	0.5	2.0000	HTI NW-4	24	0
6	KCl	5.0	2.0045	HTI NW-4	24	0
7	$CaCl_2$	0.5	1.3335	10 nm NCAM	24	0
8	$CaCl_2$	5.0	1.3380	10 nm NCAM	24	0
9	$CaCl_2$	0.5	1.3335	HTI ES-2	24	0
10	$CaCl_2$	5.0	1.3380	HTI ES-2	24	0
11	$CaCl_2$	0.5	1.3335	HTI NW-4	24	0
12	$CaCl_2$	5.0	1.3380	HTI NW-4	24	0
13	KCl	0.5	2.0000	10 nm NCAM	24	10
14	KCl	5.0	2.0045	10 nm NCAM	24	10
15	KCl	0.5	2.0000	HTI ES-2	24	10
16	KCl	5.0	2.0045	HTI ES-2	24	10
17	KCl	0.5	2.0000	HTI NW-4	24	10
18	KCl	5.0	2.0045	HTI NW-4	24	10
19	$CaCl_2$	0.5	1.3335	10 nm NCAM	24	10
20	$CaCl_2$	5.0	1.3380	10 nm NCAM	24	10
21	$CaCl_2$	0.5	1.3335	HTI ES-2	24	10
22	$CaCl_2$	5.0	1.3380	HTI ES-2	24	10
23	$CaCl_2$	0.5	1.3335	HTI NW-4	24	10
24	$CaCl_2$	5.0	1.3380	HTI NW-4	24	10

Regardless of the effect of HA, the water flux of the experiments was expected to decline due to three main factors: (i) the build-up of a hydrostatic pressure head (a constraint of the system design); (ii) the decreasing osmotic pressure difference across the membrane as the experiments tended to equilibrium (physical constraint); and (iii) concentration polarization (a physical constraint of FO membranes). As such, it was necessary to run an identical baseline

experiment with zero concentration of HA for every HA experiment to determine the water flux behavior without the presence of HA.

2.1.2 HA Feed Solution

The goal in developing the HA FS mixing procedure was to create a solution that represented to a close degree natural solutions within which the membranes are used. As such limited pre-filtering was the only form of purification used. All HA feed solutions were mixed to a concentration of 10 mg/L ±0.5 mg/L and used technical grade 53680 HA from Sigma Aldrich (St. Louis, MO). The appropriate amount of HA and background electrolyte were measured using an OHAUS Explorer Pro analytical balance and combined with the appropriate amount of deionized (18.2 MΩ/cm @ 25°C) water from a Millipore Driect-Q UV system. The solution was sonicated (Branson 3510) for five minutes and then stirred on a magnetic stirring plate at 700 rpm for 24 hours ±1 hour. Finally, the solution was filtered with Whatman grade 1 (11 μm) filter paper.

2.1.3 Electrolyte Feed and Draw Solutions

Electrolyte feed and draw solutions were mixed by measuring out the appropriate amount of electrolyte and combining it with the appropriate amount of deionized water. The solutions were then stirred on a magnetic stirring plate at 500 rpm for 10 minutes. Potassium chloride (KCl) P3911 and calcium chloride dehydrate ($CaCl_2 \cdot 2H_20$) 223506 from Sigma Aldrich were used.

2.1.4 Membranes

Three different membranes were used in the HA fouling experiments; see Figure 2.5. Nanocapillary array membranes (NCAMs) from GE Osmonics (Minnetonka, MN) with a nominal pore size of 10 nm and a nominal pore density of 6×10^8 pores/cm^2 were used. NCAMs are polycarbonate track-etched membranes coated with polyvinyl pyrrolidone to enhance

hydrophilicity of the pores. NCAMs were pretreated by soaking in the membrane in deionized water for 48 hours and then in the background electrolyte for four hours. NCAMs were always oriented such that the shiny or more hydrophobic side of the membrane was towards the DS.

Forward osmosis membranes were provided by Hydration Technologies Innovations (HTI) (Scottsdale, AZ). Membrane 081118-ES-2 (ES-2) is a cellulose triacetate with an embedded polyester screen mesh and is used in HTI's cartridge products with the DS away from the rejection layer; see Figure 2.3. With the rejection layer towards a 45% glucose draw solution at 20°C pure water fluxes of 13 - 17 L/m^2-hour are typical, with higher fluxes into concentrated salt solutions. Sodium chloride rejections range from 93-95% [16].

Membrane 101013-NW-4 (NW-4) is a cellulose triacetate cast onto a non-woven backing consisting of polyester fibers individually coated with polyethylene. NW-4 is used in HTI's pouch products which include hydration bags for various emergency and outdoor applications, generally with the FS away from the rejection layer, see Figure 2.4. With the rejection layer towards a 45% glucose draw solution at 20°C pure water fluxes of 10 - 14 L/m^2-hour are typical, with higher fluxes into concentrated salt solutions. Sodium chloride rejections range from 95-97% [16]. This information is summarized in Table 2.2. For both ES-2 and NW-4, water flux is always higher with rejection layer towards the DS [16]. ES-2 and NW-4 membranes were pretreated by soaking the membrane in deionized water for thirty minutes immediately before use, as directed by the manufacturer. Membranes were then transferred from the deionized water to the apparatus and were submerged in the working solutions, a process that took 1 ± 0.5 minutes. It was important that the membranes do not dry out as this causes the pores to collapse, known as "osmotic deswelling", significantly decreasing flux [8, 16]. Both ES-2 and NW-4

membranes were oriented such that the rejection layer was towards the DS. This was done in an effort to obtain higher fluxes and therefore a more noticeable fouling effect.

Table 2.2: Forward osmosis membrane summary. Note: flux was quantified using a pure water feed solution into a 45% glucose draw solution at 20°C.

Membrane	Active material	Support material	Coating	Flux (L/m^2-hour)	NaCl rejection (%)	Application
ES-2	Cellulose triacetate	Polyester screen mesh	None	13 – 17	93-95	Cartridge
NW-4	Cellulose triacetate	Polyester fibers	Polyethylene	10 – 14	95-97	Pouch

Figure 2.3: Example of HTI's spiral-wound cartridge products [16].

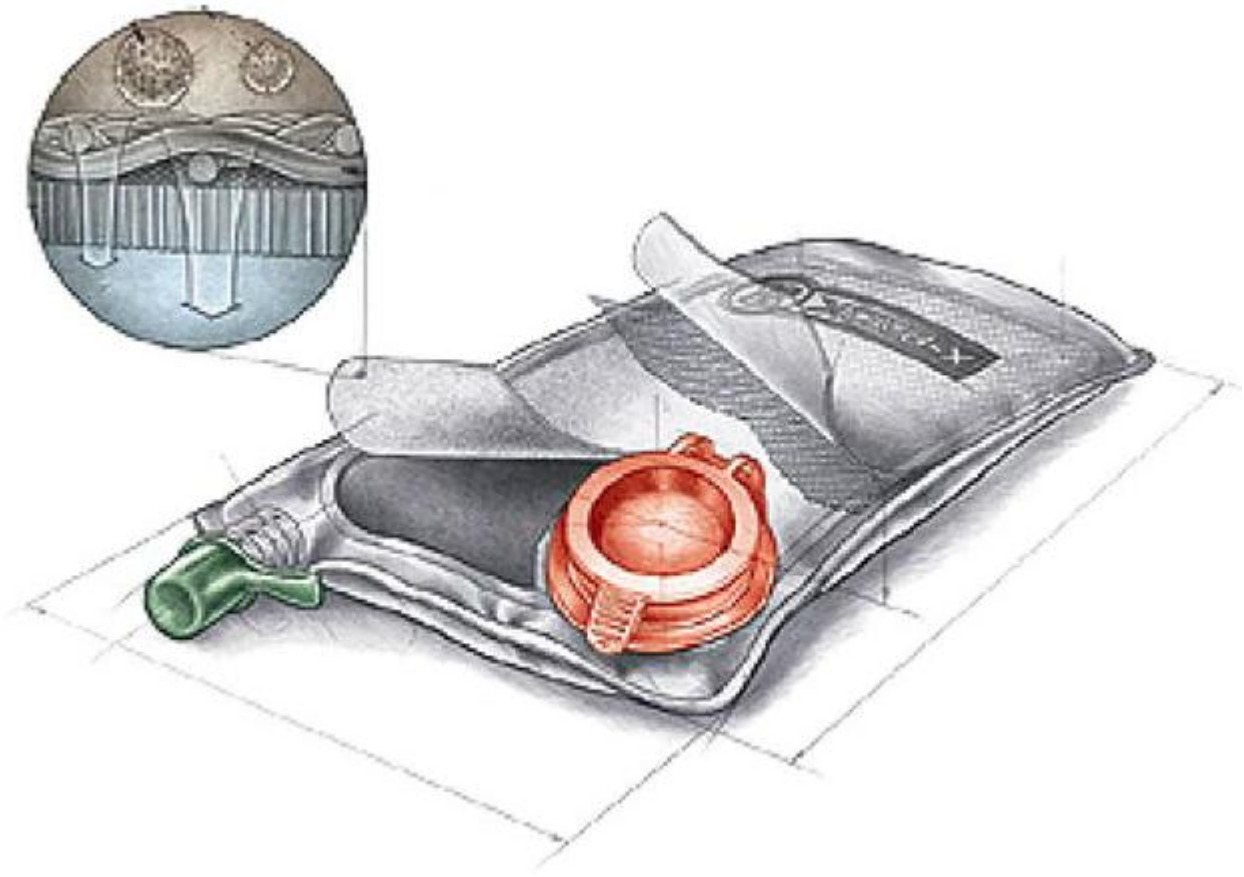

Figure 2.4: Schematic of a hydration pack [8].

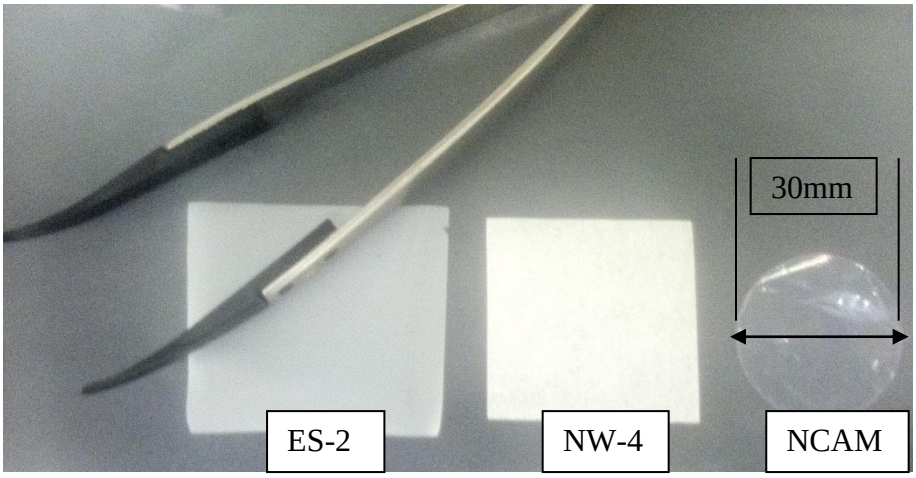

Figure 2.5: Photo of membranes used for HA experiments.

3. Results and Discussion

3.1 Effect of Ionic Strength on Water Flux

Average trans-membrane water flux was calculated at each point by using Equation 3-1. The 10 nm NCAM membrane allowed for diffusion of the KCl from the draw solution to the feed solution and did not produce measurable a flow of water in the test duration of 24 hours. Additionally, no film or foulant layer was visible macroscopically nor with the optical microscope for the NCAMs. As such, no flux was calculated for the NCAM experiments and the NCAM experiments with $CaCl_2$ were not pursued.

$$\bar{J}_n = \frac{V_{t_0} - V_{t_n}}{A[t_0 - t_n]} \qquad 3\text{-}1$$

$\bar{J}_n$ = average water flux toward DS at time *n*

$V_{t_{0,n}}$ = volume of FS at time zero, *n*

A = area of membrane

t_0, t_n = time of measurement

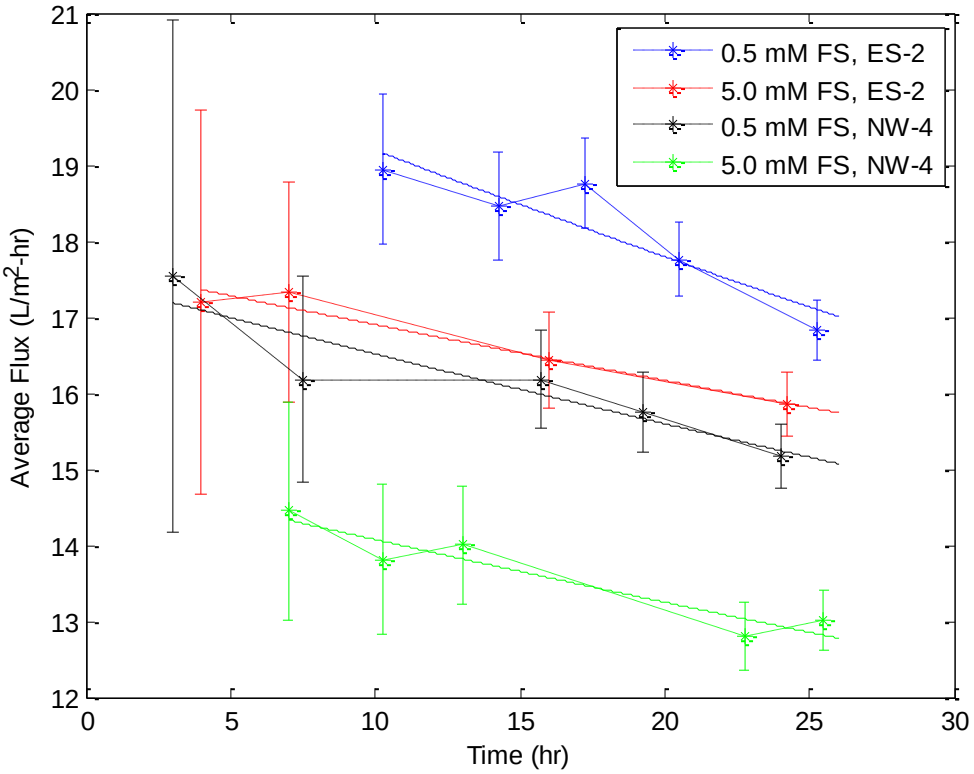

Figure 3.1: Effect of ionic strength of feed solution on average flux through ES-2 and NW-4 membranes for KCl working solutions in the presence of 10 mg/L HA in feed solution. Data was fit with curves of the form $\bar{J} = ae^{bt}$. Draw solutions were adjusted to give equivalent nominal trans-membrane osmotic pressure differences to permit the same nominal driving force.

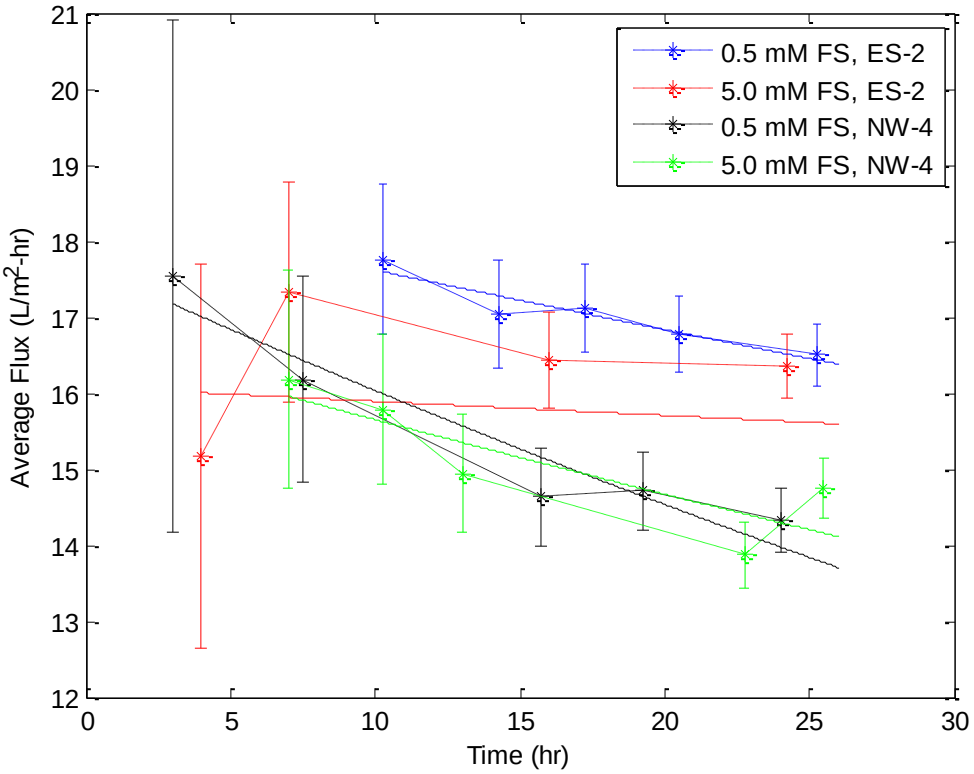

Figure 3.2: Effect of ionic strength of feed solution on average flux through ES-2 and NW-4 membranes for KCl working solutions in the presence of 0 mg/L HA in feed solution. Data was fit with curves of the form $\bar{J} = ae^{bt}$. Draw solutions were adjusted to give equivalent nominal trans-membrane osmotic pressure differences to permit the same nominal driving force.

Figure 3.1 and Figure 3.2 show the effect of ionic strength of KCl feed solutions on the average trans-membrane water flux both in the presence of humic acid and without humic acid, respectively. In both cases, the 0.5 mM feed solutions produced higher average fluxes compared to the 5.0 mM feed solutions. It should be noted that throughout the experiment there was overlap due to the uncertainty in the measurement, however in each instance the measured initial average flux was always greater for the 0.5 mM feed solutions compared to the 5.0 mM feed solutions. The initial average fluxes of the 0.5 mM feed solutions were 2.2 L/m^2-hr greater than those of the 5.0 mM feed solutions. This average flux trend was consistent across both types of forward osmosis membranes, ES-2 and NW-4.

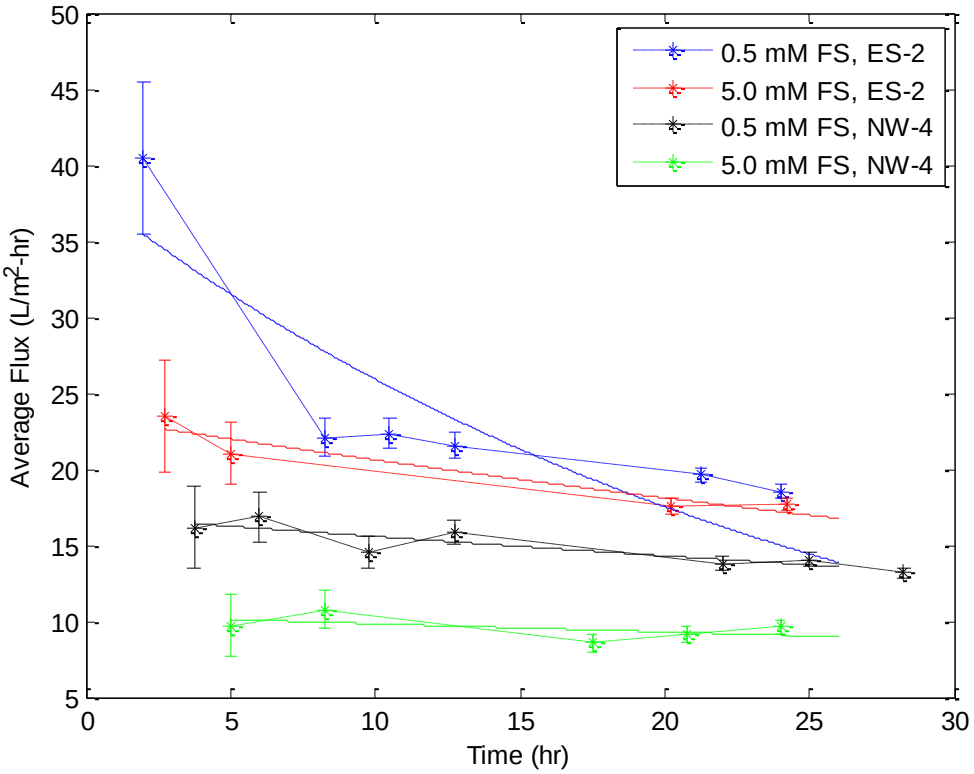

Figure 3.3: Effect of ionic strength of feed solution on average flux through ES-2 and NW-4 membranes for $CaCl_2$ working solutions in the presence of 10 mg/L HA in feed solution. Data was fit with curves of the form $\bar{J} = ae^{bt}$. Draw solutions were adjusted to give equivalent nominal trans-membrane osmotic pressure differences to permit the same nominal driving force.

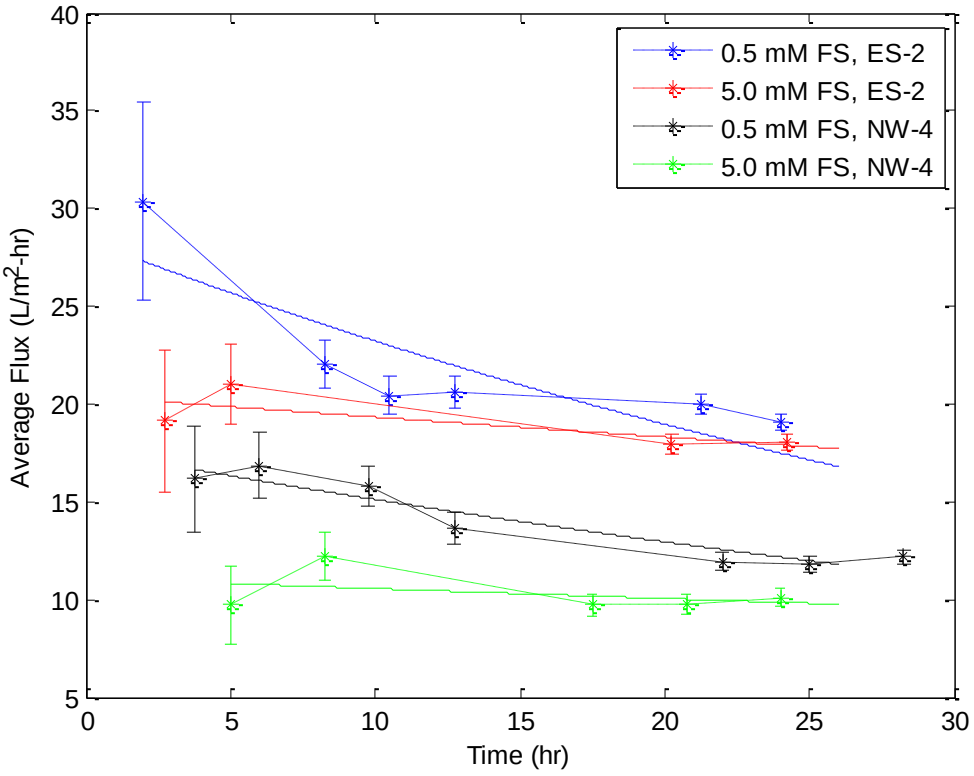

Figure 3.4: Effect of ionic strength of feed solution on average flux through ES-2 and NW-4 membranes for $CaCl_2$ working solutions in the presence of 0 mg/L HA in feed solution. Data was fit with curves of the form $\bar{J} = ae^{bt}$. Draw solutions were adjusted to give equivalent nominal trans-membrane osmotic pressure differences to permit the same nominal driving force.

Figure 3.3 and Figure 3.4 show the effect of ionic strength of $CaCl_2$ feed solutions on the average trans-membrane water flux both in the presence of humic acid and without humic acid, respectively. In both cases, the 0.5 mM feed solutions produced higher average fluxes at all times compared to the 5.0 mM feed solutions. The initial average fluxes of the 0.5 mM feed solutions were 10. L/m^2-hr greater than those of the 5.0 mM feed solutions. This was consistent across both types of forward osmosis membranes, ES-2 and NW-4.

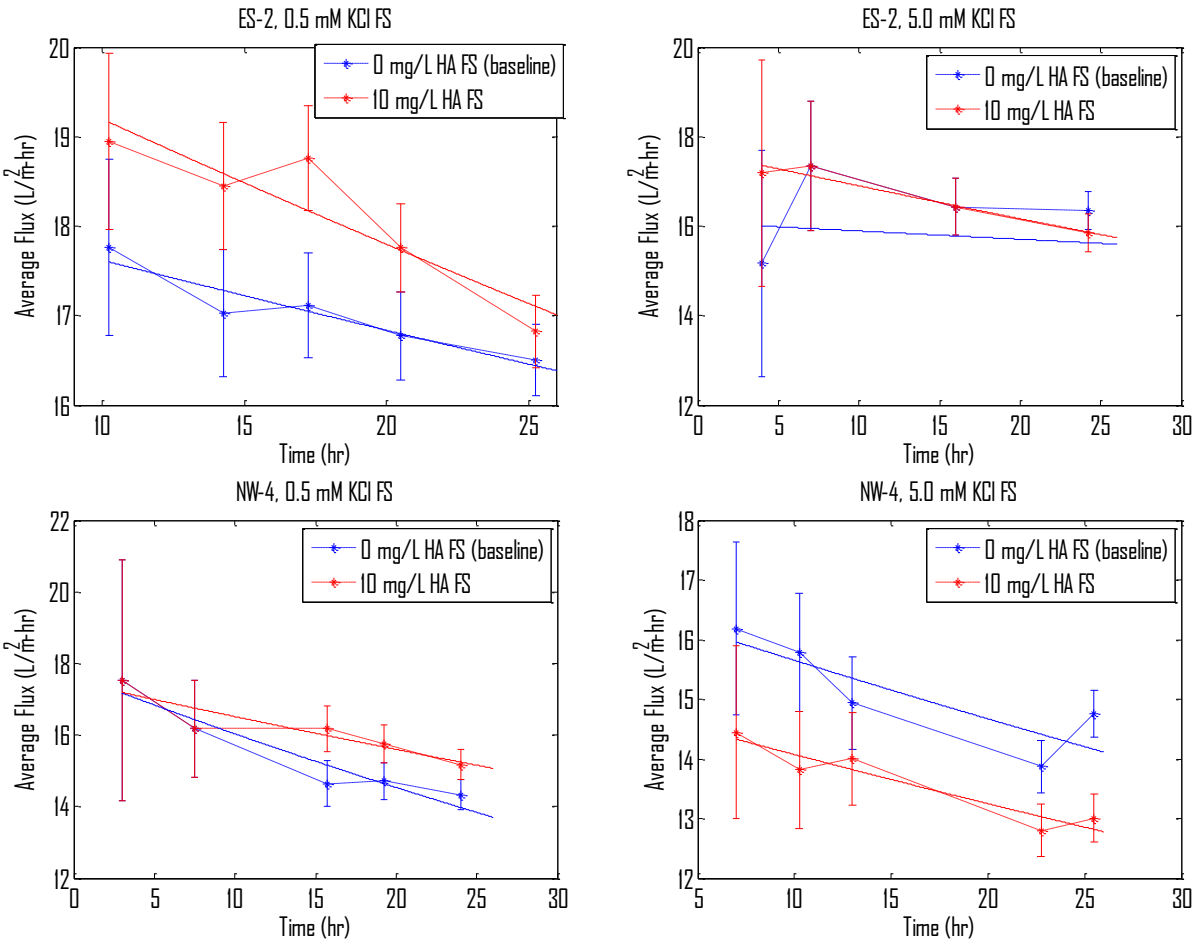

Figure 3.5: Effect of 10 mg/L HA FS in KCl working solutions on average flux through both membrane ES-2 and membrane NW-4. Data was fit with curves of the form $\bar{J} = ae^{bt}$.

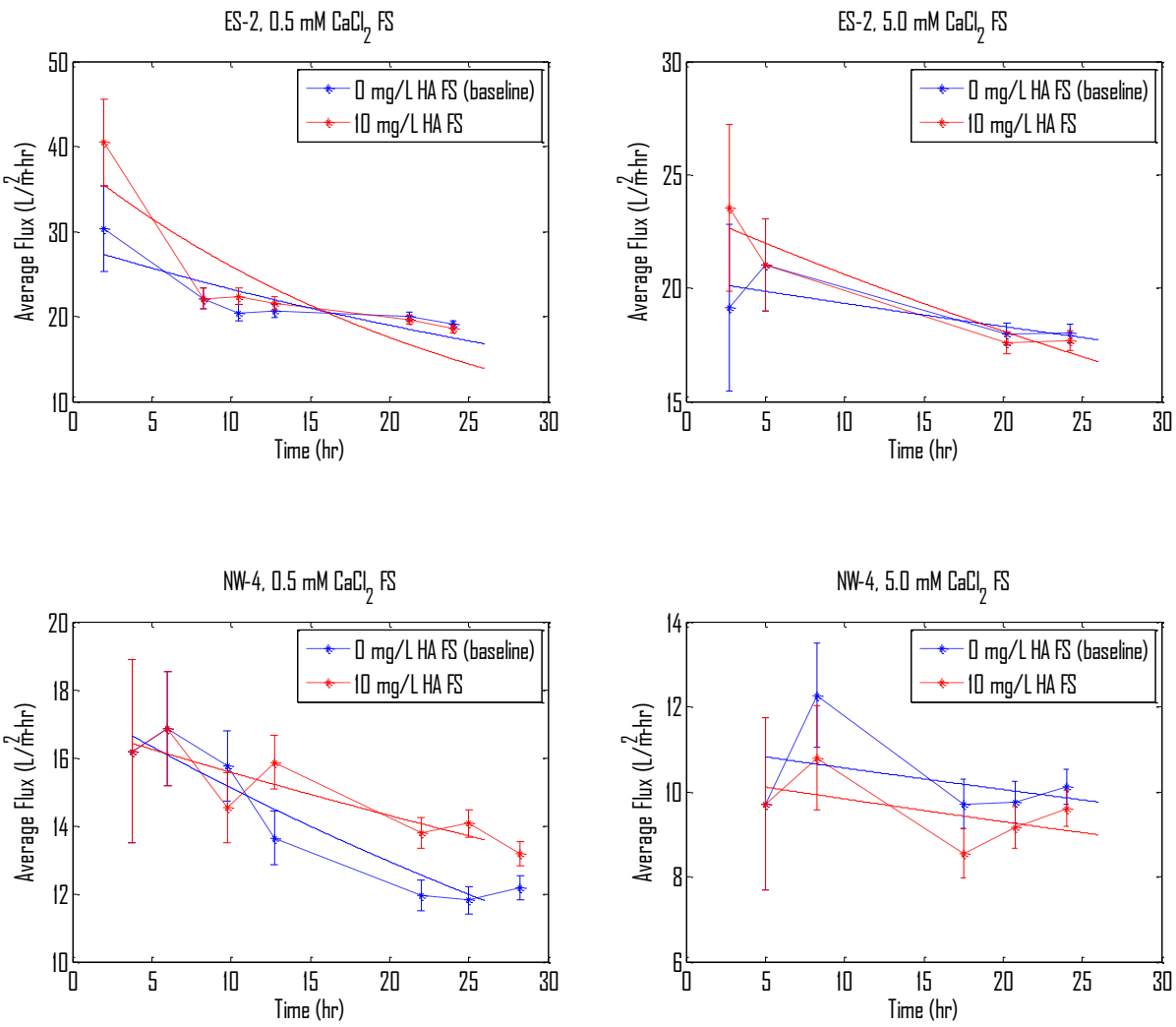

Figure 3.6: Effect of 10 mg/L HA FS in $CaCl_2$ working solutions on average flux through both membrane ES-2 and membrane NW-4. Data was fit with curves of the form $\bar{J} = ae^{bt}$.

Figure 3.5 and Figure 3.6 show the effect of 10 mg/L HA in feed solutions for both KCl and $CaCl_2$ working solutions. The value of the curve fit coefficient *b* physically represents the rate at which the average flux decays with time. To quantify the effect of HA on average flux the average value of the coefficient *b* for the baseline experiments and the HA experiments was calculated; see Table 1.1. b_{avg} for the baseline experiments is greater than b_{avg} for the humic acid experiments meaning that the average flux of the baseline experiments decayed slower on

average. This would imply that HA fouling was at least partially responsible for the average flux declines but it is unsure to what extent.

Table 3.1: Average value of *b* coefficient for baseline and humic acid experiments.

Experiment	b_{avg} (hr^{-1})
Baseline	-0.0085
Humic acid	-0.0112

The ionic strength of the feed solution was shown to play a significant role in the average trans-membrane water flux. Regardless of salt type, membrane type, and humic acid concentration, the 0.5 mM feed solution produced larger fluxes than the 5.0 mM feed solution; see Figure 3.1, Figure 3.2, Figure 3.3, and Figure 3.4. Higher ionic strengths have been shown to promote fouling by screening the electrostatic repulsion between the HA molecule and the membrane. This is achieved when counter ions in the electrolyte surround the membrane and molecule and decrease the effect of the electric double layer [13]. In addition, higher ionic strengths have also been shown to increase internal concentration polarization and lead to osmotic deswelling of the membrane pores, resulting in flux declines [8]. The problem now becomes one of determining to what extent each mechanism is responsible for the decreased flux at higher ionic strengths of the feed solutions.

To determine if the decrease in average trans-membrane water flux at higher ionic strengths was due to internal concentration polarization or HA fouling it was necessary to compare the average fluxes of baseline experiments with those containing 10 mg/L HA; see Figure 3.5 and Figure 3.6. As discussed earlier, the effect of HA fouling on the average trans-membrane water flux was not measurable relative to the baseline experiments. Since the effect

of HA fouling on the average flux was not measurable, this implies that the primary reason for the measurable decrease in average fluxes at higher ionic strengths of feed solutions was due to internal concentration polarization and not HA fouling.

3.2 Effect of Salt Type on Water Flux

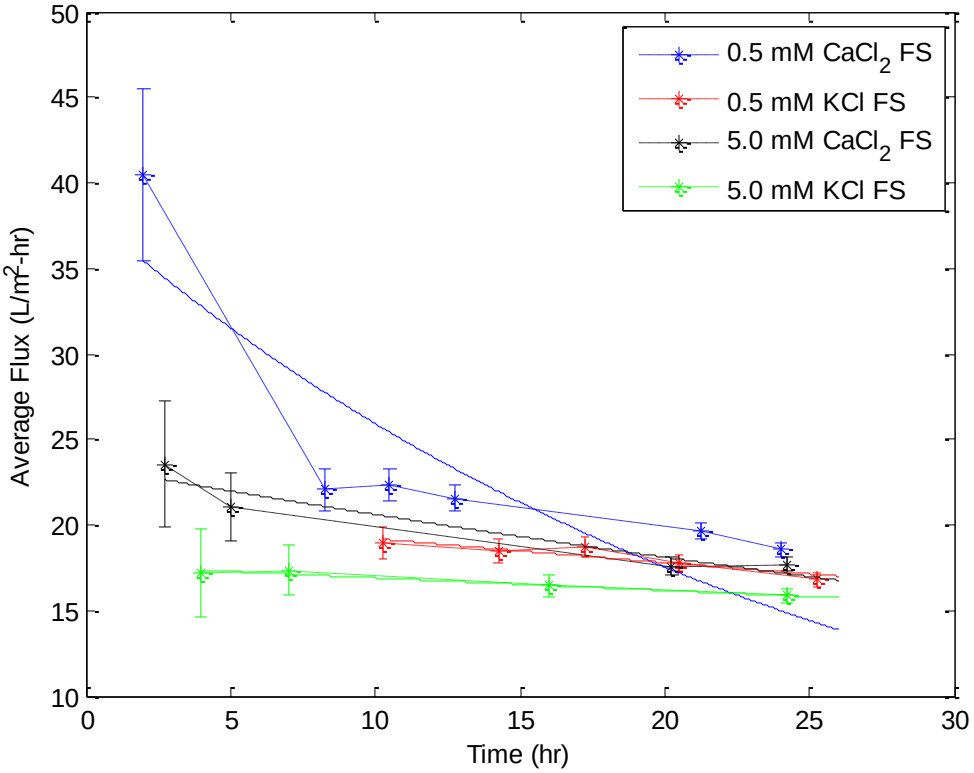

Figure 3.7: Effect of salt type on average flux through ES-2 membrane for $CaCl_2$ and KCl working solutions in the presence of 10 mg/L HA in feed solution. Data was fit with curves of the form $\bar{J} = ae^{bt}$. Draw solutions were adjusted to give equivalent nominal trans-membrane osmotic pressure differences to permit the same nominal driving force.

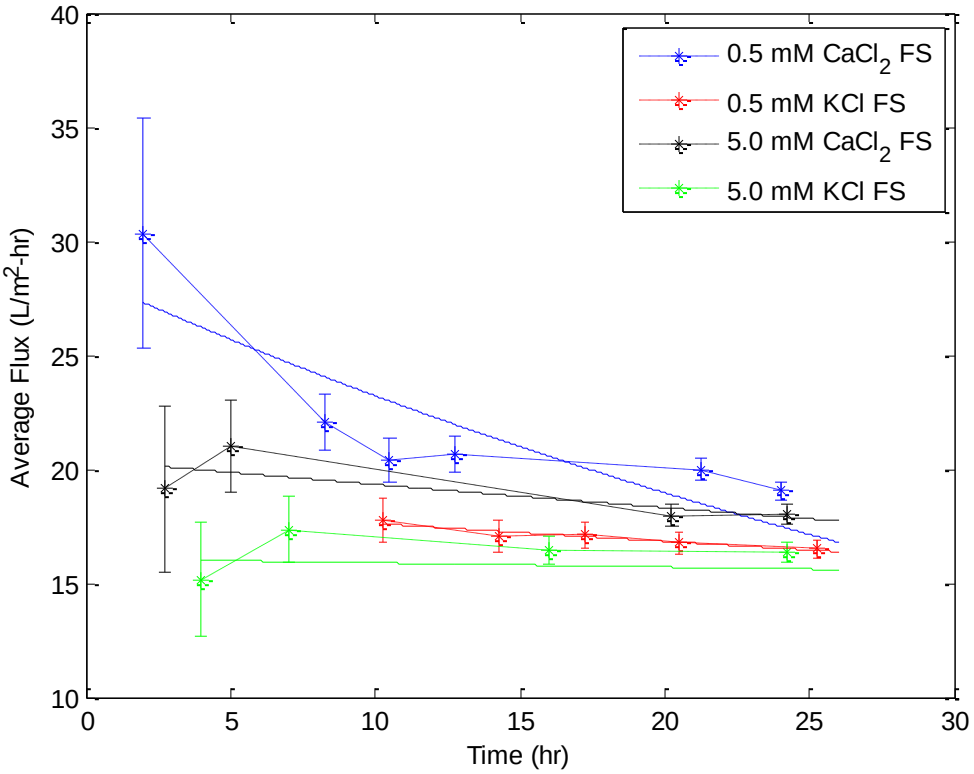

Figure 3.8: Effect of salt type on average flux through ES-2 membrane for $CaCl_2$ and KCl working solutions in the presence of 0 mg/L HA in feed solution. Data was fit with curves of the form $\bar{J} = ae^{bt}$. Draw solutions were adjusted to give equivalent nominal trans-membrane osmotic pressure differences to permit the same nominal driving force.

Figure 3.7 and Figure 3.8 show the effect of salt type on the average trans-membrane water flux across membrane ES-2 both in the presence of humic acid and without humic acid, respectively. In both cases, the $CaCl_2$ working solutions produced higher average fluxes compared to the KCl working solutions for a given feed solution ionic strength. $CaCl_2$ working solutions produced an average initial flux 11 L/m^2-hr greater than that for KCl working solutions.

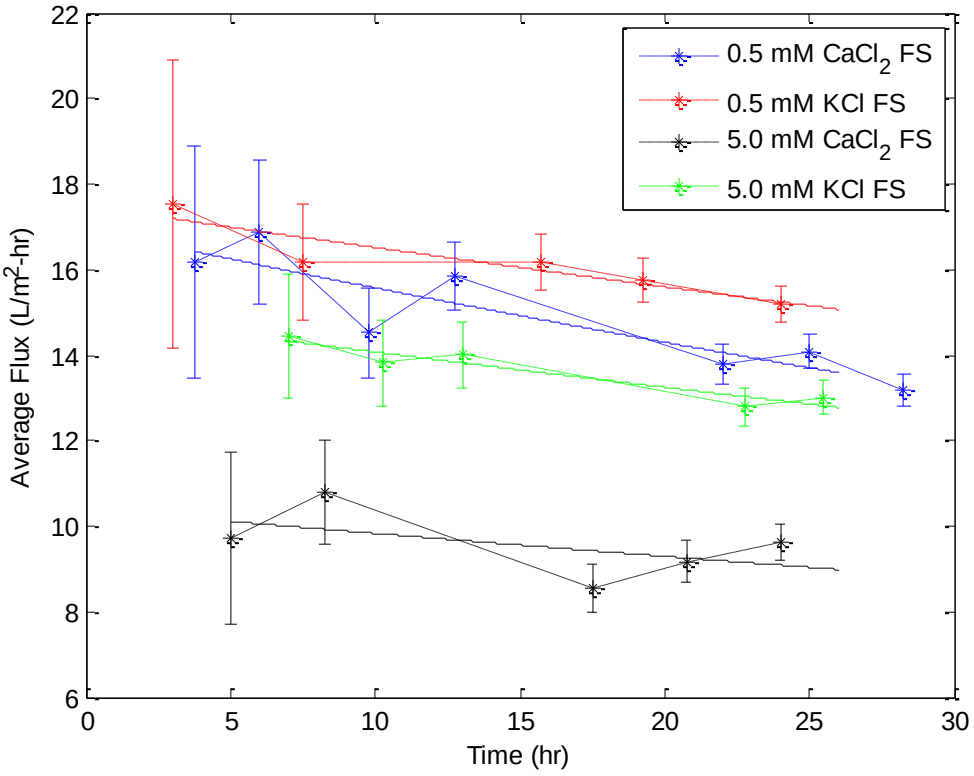

Figure 3.9: Effect of salt type on average flux through NW-4 membrane for $CaCl_2$ and KCl working solutions in the presence of 10 mg/L HA in feed solution. Data was fit with curves of the form $\bar{J} = ae^{bt}$. Draw solutions were adjusted to give equivalent nominal trans-membrane osmotic pressure differences to permit the same nominal driving force.

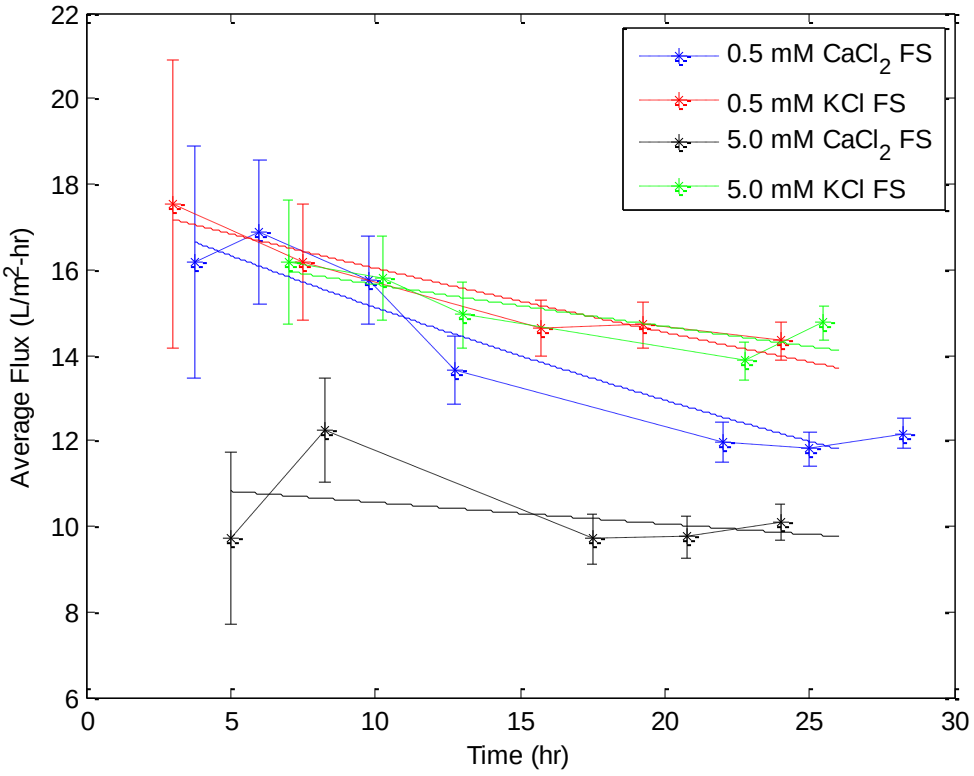

Figure 3.10: Effect of salt type on average flux through NW-4 membrane for $CaCl_2$ and KCl working solutions in the presence of 0 mg/L HA in feed solution. Data was fit with curves of the form $\bar{J} = ae^{bt}$. Draw solutions were adjusted to give equivalent nominal trans-membrane osmotic pressure differences to permit the same nominal driving force.

Figure 3.9 and Figure 3.10 show the effect of salt type on the average trans-membrane water flux across membrane NW-4 both in the presence of humic acid and without humic acid, respectively. Contrary to membrane ES-2, the KCl working solutions produced higher average fluxes compared to the $CaCl_2$ working solutions for a given feed solution ionic strength. For membrane NW-4, KCl working solutions produced an average initial flux that was 3.5 L/m^2-hr greater than that for $CaCl_2$ working solutions. It should be noted that throughout the experiment there was overlap due to the uncertainty in the measurement, however in each instance the measured initial average flux was always greater for the KCl working solutions compared to the $CaCl_2$ working solutions.

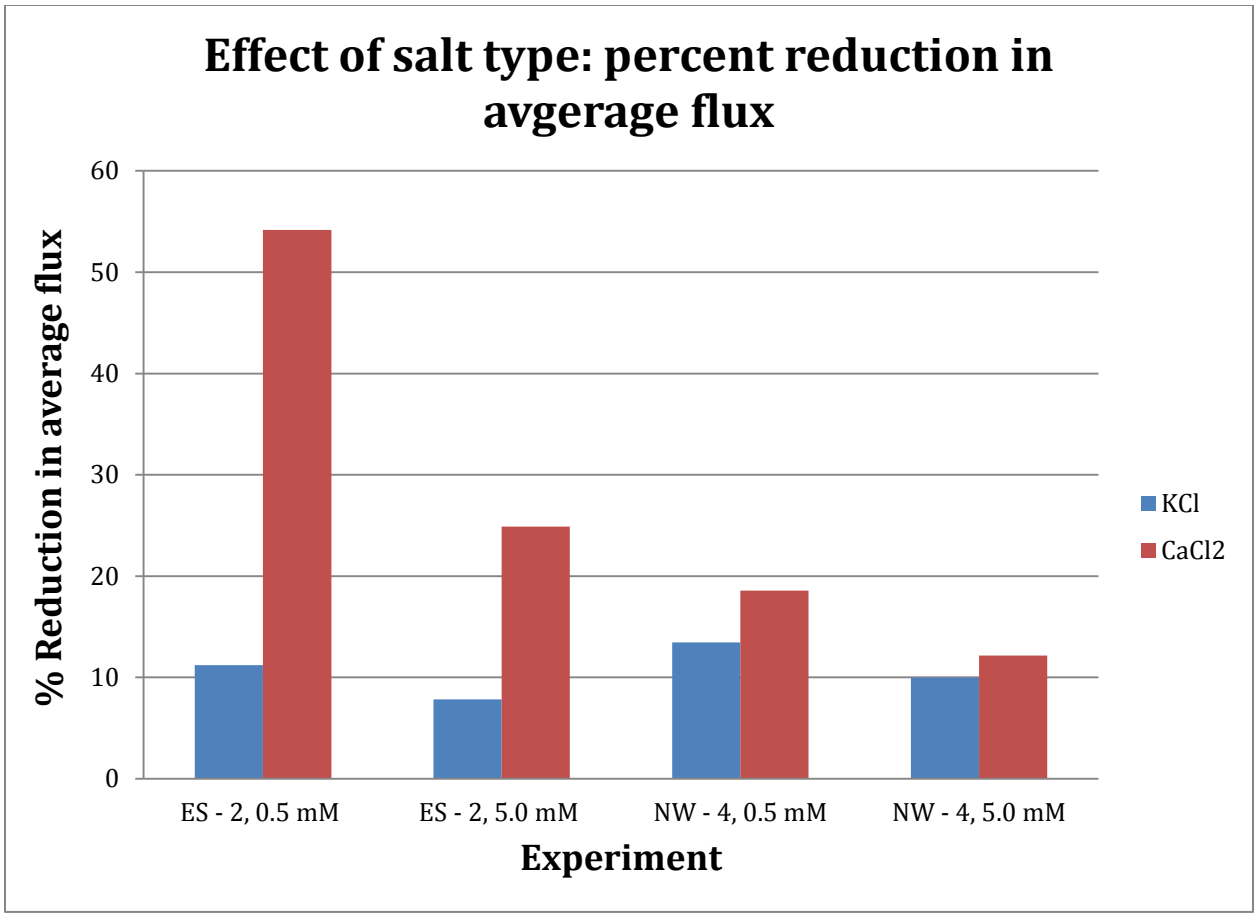

Figure 3.11: Percent reduction of average flux for KCl and $CaCl_2$ working solutions in the presence of 10 mg/L HA for all four different experimental conditions. The percent reduction is shown on the vertical axis for each experimental condition shown on the horizontal axis. Note: the plot does not account for differences in time of initial and final measurements when calculating percent reductions (initial flux measurements were taken at 6 ± 4.25 hours, final flux measurements were taken at 26 ± 2.25 hours).

Figure 3.11 shows the effect of salt type on the percent reduction of average water flux from the initial measurement to the final measurement. Percent reduction was calculated from Equation 3-2. In all cases $CaCl_2$ had larger percent reductions in flux, but this margin decreases at higher ionic strengths and for membrane NW-4.

$$\%\mathbf{R} = \frac{\bar{J}_i - \bar{J}_f}{\bar{J}_i} \qquad 3\text{-}2$$

%R = percent reduction

$\overline{J_i}$ = initial flux

$\overline{J_f}$ = final flux

For membrane ES-2, $CaCl_2$ working solutions produced larger fluxes than KCl; see Figure 3.7 and Figure 3.8. This could suggest that although the nominal osmotic pressure differences were equal, perhaps the actual driving osmotic pressure difference of $CaCl_2$ working solutions was greater than that of the KCl solutions due to ion pairing or other salt-dependent effects. However, for membrane NW-4, KCl working solutions produced an average initial flux that was greater than that for $CaCl_2$ working solutions; see Figure 3.9 and Figure 3.10. These two contradictory results imply that the effect of salt type on average flux is membrane dependent since the same feed and draw solutions (and therefore same nominal osmotic pressure difference) were used for both membranes.

To determine the effect of salt type on HA fouling the percent reduction in average flux was calculated for each experiment; see Figure 3.11. For membrane ES-2, $CaCl_2$ working solutions had average flux reductions at least 17% greater than KCl working solutions for both feed solution concentrations. It could be argued that the larger percent reductions in average flux for $CaCl_2$ working solutions were a result of increased HA fouling due to the larger initial average fluxes of these solutions. However, we see the same result for membrane NW-4, as $CaCl_2$ working solutions had flux reductions at least 2.2% greater than KCl working solutions for both feed solution concentrations. This result refutes the argument that the larger percent reductions in average flux through membrane ES-2 for $CaCl_2$ working solutions were solely a result of the larger initial average fluxes of $CaCl_2$ working solutions. This is because for membrane NW-4 KCl working solutions produced larger initial average fluxes while still having lesser percent flux reductions than $CaCl_2$ working solutions. Thus, larger percent flux reductions were found using $CaCl_2$ working solutions compared to KCl working solutions regardless of

which working solution produced the larger initial average flux. This larger percent reduction should be due at least in part to increased HA fouling of the membranes in the presence of Ca^{2+} ions.

Figure 3.12, Figure 3.13, Figure 3.14, and Figure 3.15 show digital photographs of membrane ES-2 taken with an optical microscope at 40X zoom. For both KCl and $CaCl_2$ working solutions, HA build-up is visible on the support surface of the membrane (the side facing the FS). Complete discoloration was observed for some sections of ES-2 for the $CaCl_2$ working solution while this was never observed for the KCl working solution; see Figure 3.13 and Figure 3.15. Although no HA layer is visible, Figure 3.16, Figure 3.17, Figure 3.18, and Figure 3.19 showing digital photographs of membrane NW-4 were included for completeness. Figure 3.20 shows digital a photograph of membranes ES-2 and NW-4 post experiment.

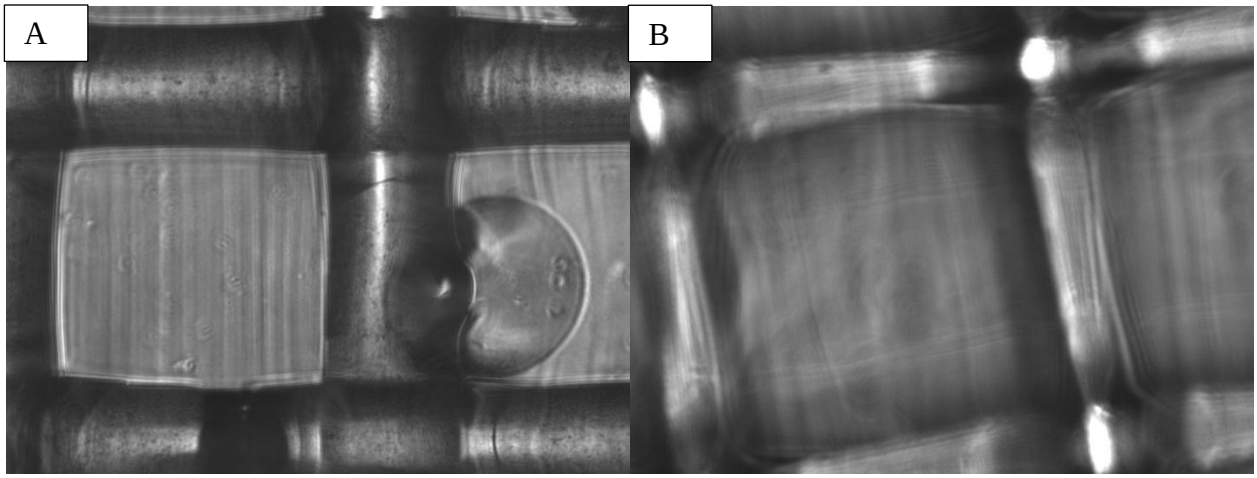

Figure 3.12: ES-2 membrane immediately after experiment: 0.5 mM KCL, 0 mg/L HA FS. A.) DS side; B.) FS side

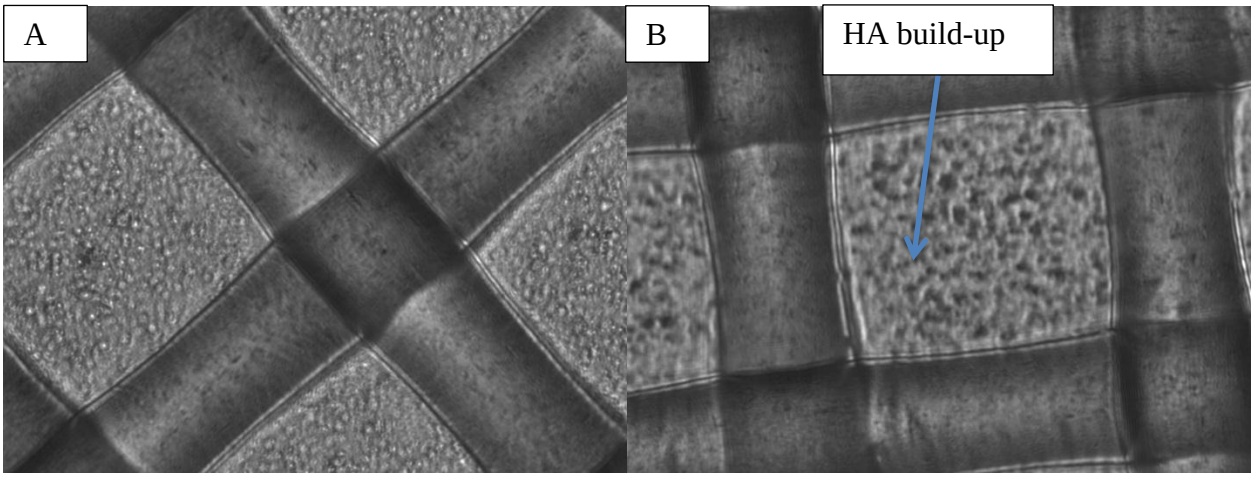

Figure 3.13: ES-2 membrane immediately after experiment: 0.5 mM KCL, 10 mg/L HA FS. A.) DS side; B.) FS side

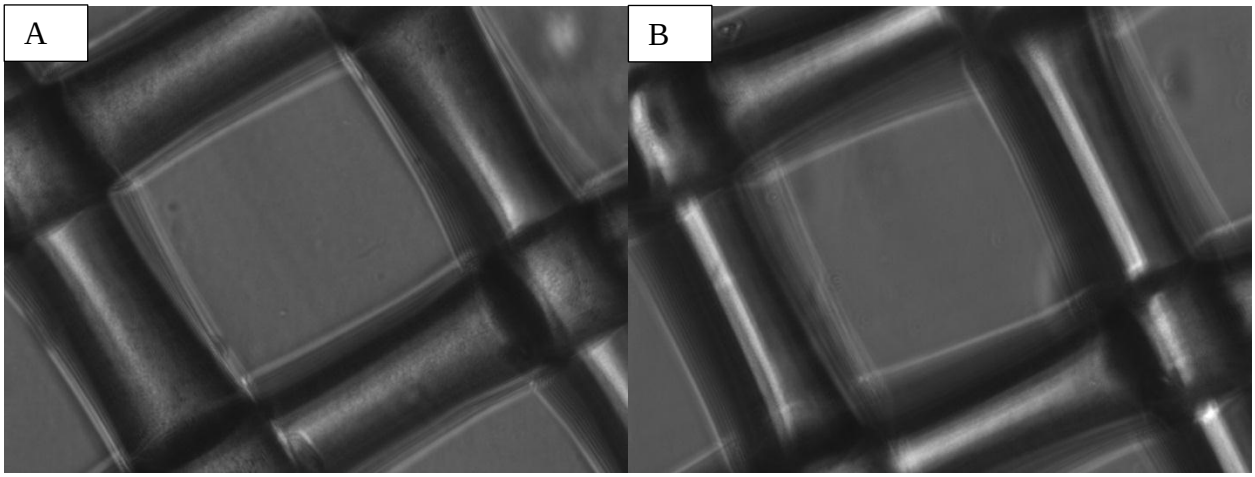

Figure 3.14: ES-2 membrane immediately after experiment: 0.5 mM $CaCl_2$, 0 mg/L HA FS. A.) DS side; B.) FS side

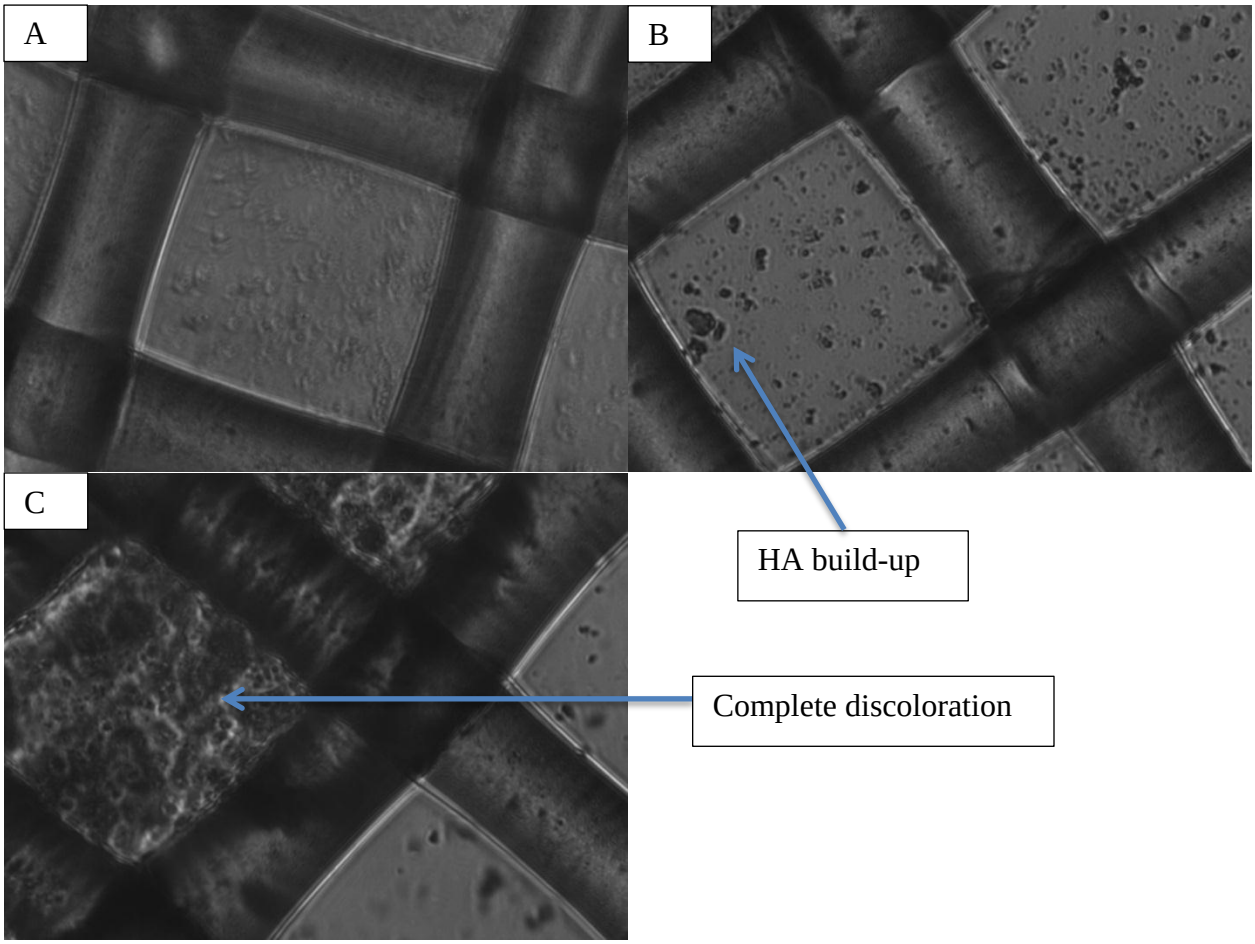

Figure 3.15: ES-2 membrane immediately after experiment: 0.5 mM $CaCl_2$, 10 mg/L HA FS. A.) DS side; B.) FS side; C.) Heavy fouling section of FS side

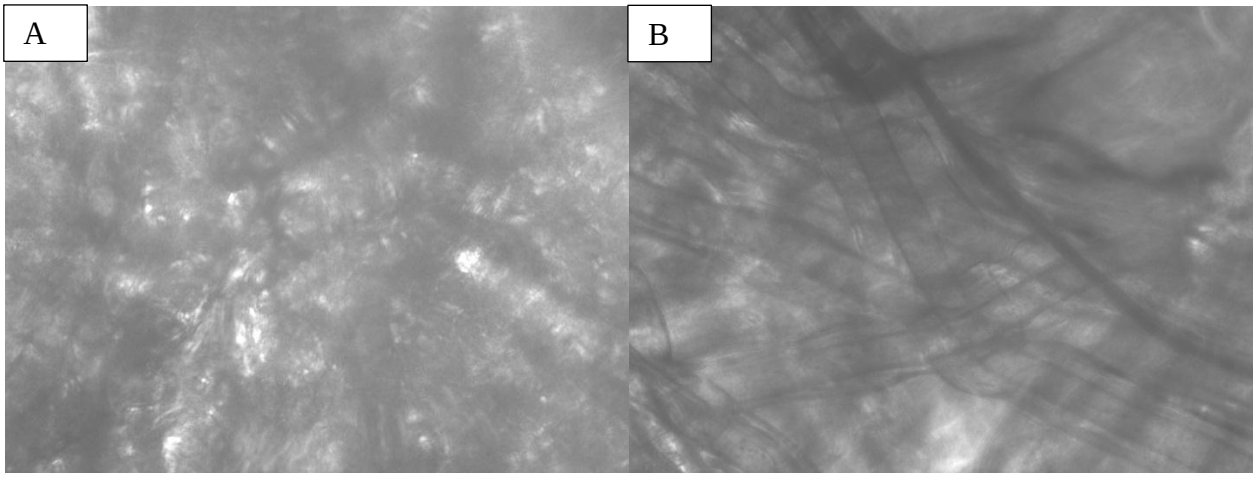

Figure 3.16: NW-4 membrane immediately after experiment: 0.5 mM KCl, 0 mg/L HA FS. A.) DS side; B.) FS side

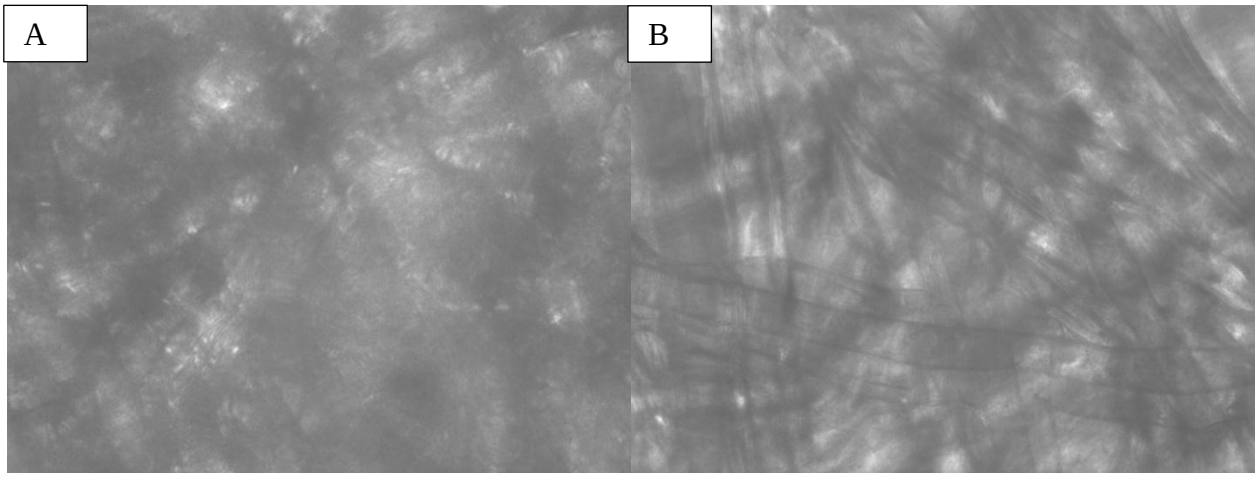

Figure 3.17: NW-4 membrane immediately after experiment: 0.5 mM KCl, 10 mg/L HA FS. A.) DS side; B.) FS side

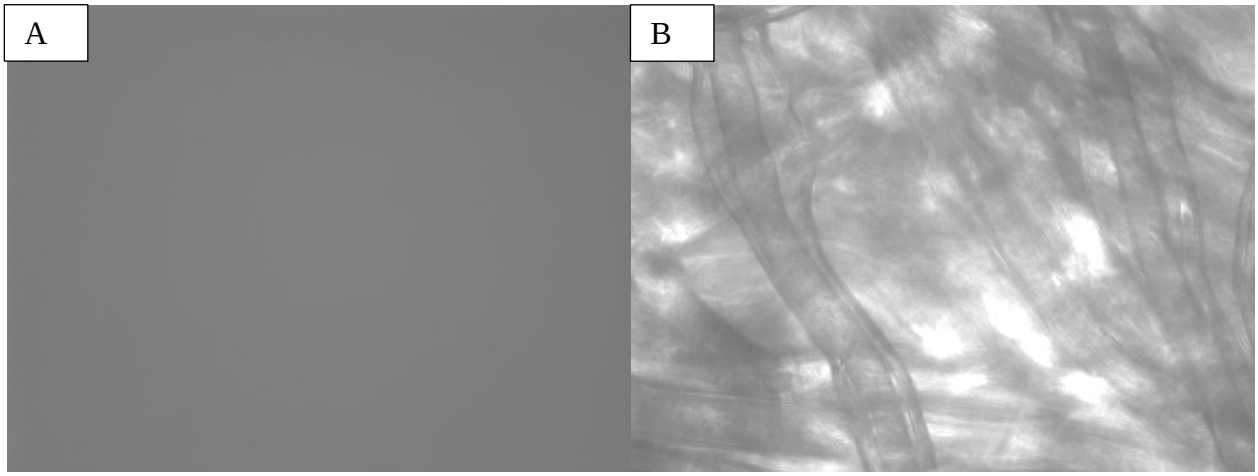

Figure 3.18: NW-4 membrane immediately after experiment: 0.5 mM $CaCl_2$, 0 mg/L HA FS. A.) DS side; B.) FS side

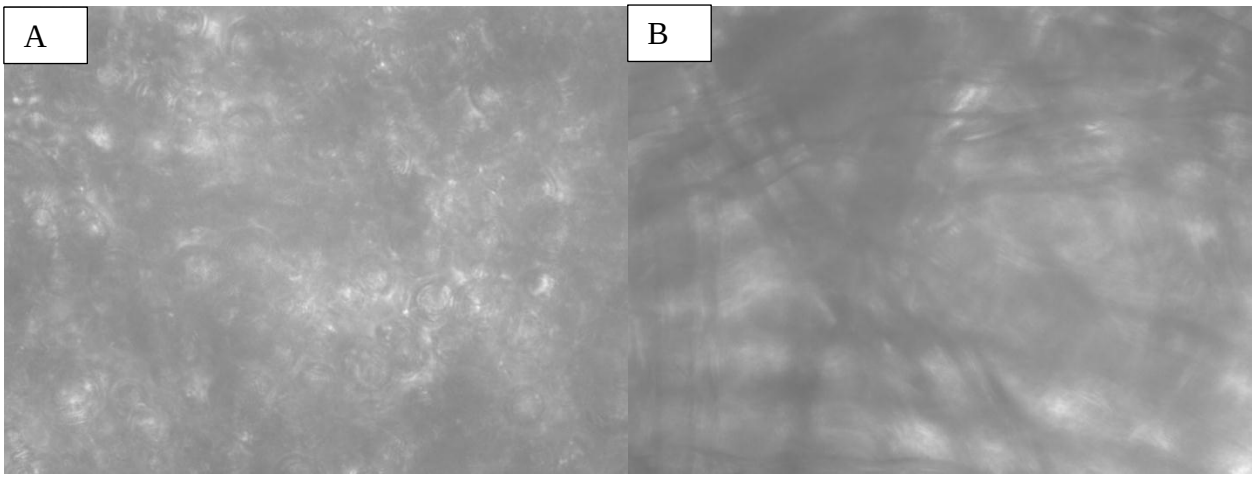

Figure 3.19: NW-4 membrane immediately after experiment: 0.5 mM $CaCl_2$, 10 mg/L HA FS. A.) DS side; B.) FS side

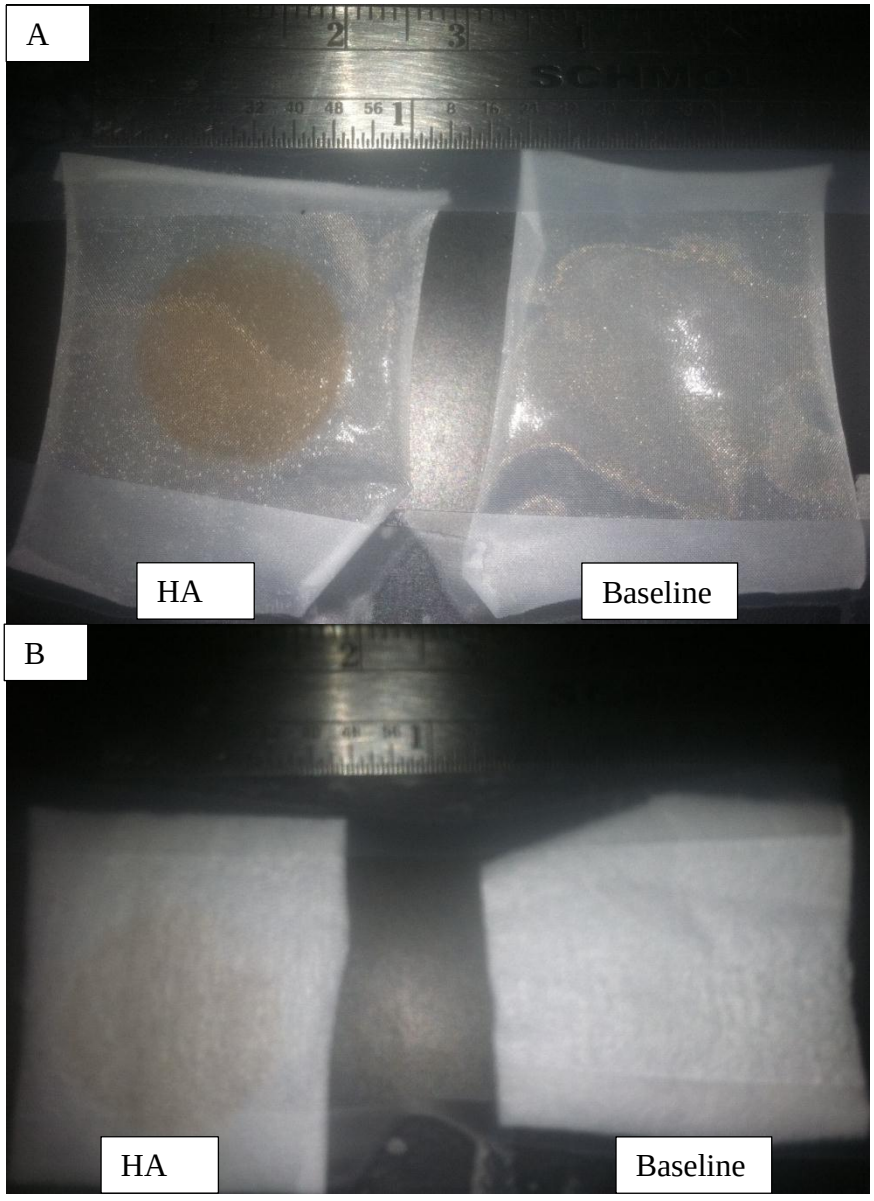

Figure 3.20: A.) Membrane ES-2, 0.5 mM KCl FS; B.) Membrane NW-4, 0.5 mM KCl FS.

4. CONCLUSION

Internal concentration polarization was shown to dominate average flux reductions at high ionic strengths while the effect of HA fouling was measurable in the presence of $CaCl_2$ working solutions. Ionic strength of the feed solution was shown to affect the average trans-membrane water flux with higher average fluxes found for the 0.5 mM feed solution compared to the 5.0 mM feed solution (2.2 L/m^2-hr greater initial average flux for KCl, 10. L/m^2-hr greater initial average flux for $CaCl_2$). This lesser average flux at high ionic strengths was attributed to internal concentration polarization as the effect of HA fouling was not measurable with respect to the baseline experiments. This is consistent with previous studies [8, 10]. Salt type was shown to systematically affect the average trans-membrane water flux and was found to be dependent on the membrane type. $CaCl_2$ working solutions produced an average initial water flux 11 L/m^2-hr greater than that for KCl working solutions for membrane ES-2, but KCl working solutions produced an average initial water flux 3.5 L/m^2-hr greater than that for $CaCl_2$ working solutions for membrane NW-4. Despite not always having higher initial average fluxes, $CaCl_2$ working solutions always resulted in larger percent reductions of average flux (greater than 17% for membrane ES-2, 2.2% for membrane NW-4) which could be evidence of increased HA fouling in the presence of Ca^{2+} ions. This result agrees with previous findings for reverse osmosis and nanofiltration membranes in a cross-flow setup [9, 12].

REFERENCES

[1] Prakash, S., 2009.

[2] United Nations Environment Programme

[3] The World Bank

[4] U.S. Environmental Protection Agency

[5] Service, R. F. Desalination Freshens Up. *Science* **313**, 1088-1090 (2006).

[6] Veolia Water Solutions & Technologies

[7] American Membrane Technology Association

[8] Cath, T. Y., Childress, A. E. & Elimelech, M. Forward osmosis: Principles, applications, and recent developments. *Journal of Membrane Science* **281**, 70-87 (2006).

[9] Tang, C. Y., Young-Nam, K. & Leckie, J. O. Fouling of reverse osmosis and nanofiltration membranes by humic acid—Effects of solution composition and hydrodynamic conditions. *Journal of Membrane Science* **290**, 86-94 (2007).

[10] Tang, C. Y. *et al.* Coupled effects of internal concentrations polarization and fouling on flux behavior of forward osmosis membranes during humic acid filtration. *Journal of Membrane Science* **354**, 123-133 (2010).

[11] Yuan, W. & Zydney, A. L. Humic acid fouling during ultrafiltration. Symposia paper presented before the Division of Environmental Chemistry, American Chemical Society (2000).

[12] Al-Amoudi, A. S. Factors affecting natural organic matter (NOM) and scaling fouling in NF membranes: A review. *Desalination* **259**, 1-10 (2010).

[13] Sparreboom, W., van den Berg, A., & Eijkel J. C. T. Principles and applications of nanofluidic transport. *Nature Nanotechnology* **4**, 713-720 (2009).

[14] Eimer, K. Energetic aspects of the fouling of MSF desalination plants with and without the use of on load ball cleaning system. *Desalination* **40**, 363-372 (1982).

[15] Turro, N. J. & Lei, X. G. Spectroscopic probe analysis of protein – surfactant interactions: the BSA/SDS system. *Langmuir* **11**, 2525-2533 (1995).

[16] Hydration Technology Innovations

[17] Conlisk, A. T. Essentials of Micro and Nanofluidics with Applications to the Biological and Chemical Sciences Version 4.0 (2010).